Lawrence Berkeley National Laboratory

Title
GLIMM'S METHOD FOR GAS DYNAMICS

Permalink
https://escholarship.org/uc/item/3hc761hw

Author
Colella, Phillip

Publication Date
1980-07-01

Lawrence Berkeley Laboratory
UNIVERSITY OF CALIFORNIA

Physics, Computer Science & Mathematics Division

GLIMM'S METHOD FOR GAS DYNAMICS

Phillip Colella

July 1980

DISCLAIMER

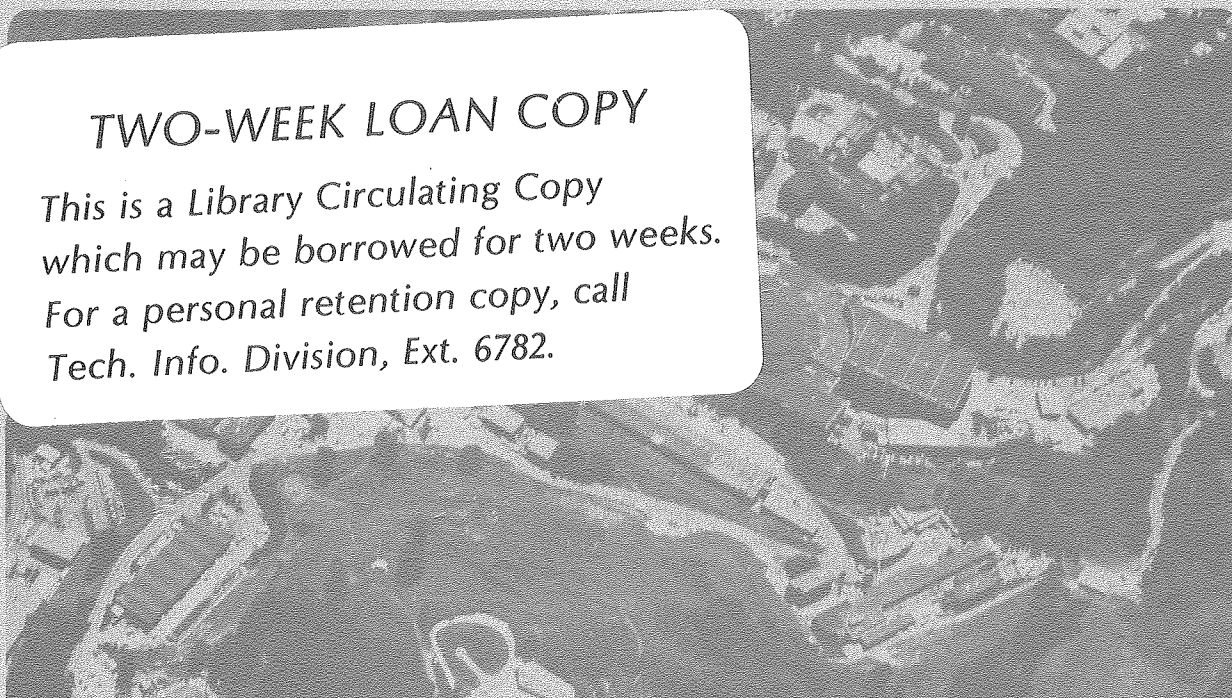This document was prepared as an account of work sponsored by the United States Government. While this document is believed to contain correct information, neither the United States Government nor any agency thereof, nor the Regents of the University of California, nor any of their employees, makes any warranty, express or implied, or assumes any legal responsibility for the accuracy, completeness, or usefulness of any information, apparatus, product, or process disclosed, or represents that its use would not infringe privately owned rights. Reference herein to any specific commercial product, process, or service by its trade name, trademark, manufacturer, or otherwise, does not necessarily constitute or imply its endorsement, recommendation, or favoring by the United States Government or any agency thereof, or the Regents of the University of California. The views and opinions of authors expressed herein do not necessarily state or reflect those of the United States Government or any agency thereof or the Regents of the University of California.

GLIMM'S METHOD FOR GAS DYNAMICS

Phillip Colella

Lawrence Berkeley Laboratory
University of California
Berkeley, California 94720

July 1980

GLIMM'S METHOD FOR GAS DYNAMICS[*]

Phillip Colella[**]

Lawrence Livermore National Laboratory
University of California
Livermore, California 94550

Abstract

We investigate Glimm's method, a method for constructing approximate solutions to systems of hyperbolic conservation laws in one space variable by sampling explicit wave solutions. It is extended to several space variables by operator splitting. We consider two functional problems. 1) We propose a highly accurate form of the sampling procedure, in one space variable, based on the van der Corput sampling sequence. We test the improved sampling procedure numerically in the case of inviscid compressible flow in one space dimension and find that it gives high resolution results both in the smooth parts of the solution, as well as the discontinuities. 2) We investigate the operator splitting procedure by means of which the multidimensional method is constructed. An O(1) error stemming from the use of this procedure near shocks oblique to the spatial grid is analyzed numerically in the case of the equations for inviscid compressible flow in two space dimensions. We present a hybrid method which eliminates this error, consisting of Glimm's method, used in continuous parts of the flow, and the nonlinear Godunov's method, used in regions where large pressure jumps are generated. The resulting method is seen to be a substantial improvement over either of the component methods for multidimensional calculations.

[**] Current address: Lawrence Berkeley Laboratory, University of California, Berkeley, California 94720.

1. INTRODUCTION

The problem which motivates this study is the numerical calculation of time-dependent, discontinuous solutions to compressible fluid flow problems in one or more space variables. There are three criteria which such approximate solutions must simultaneously satisfy.

1) The approximate solution must be reasonably accurate in regions where the flow is smooth. Continuous waves should move at the correct speed, have the correct shape, steepen or spread at the correct rate.

2) Discontinuities which are transported along characteristics should be modelled in the approximate solution by sharp jumps which are transported at the correct speed. Examples of such discontinuities are: contact discontinuities (across which the density and temperature have jump discontinuities while the pressure and velocity remain continuous); the interface between two different materials, or between two different thermodynamic phases of the same material; lines or surfaces across which the solution is continuous, but some derivative of the solution is not.

3) Nonlinear discontinuities should be computed stably and accurately. Such discontinuities occur, for example, when there is mass transported across the discontinuity, as in the case of shock fronts in an ideal gas.

The main method used for computing such solutions has been to solve a set of finite difference equations which approximate the differential equations of motion. However, it is difficult to construct difference methods which satisfy all three of the above criteria simultaneously. For example, it is well-known that a high order difference method may generate oscillations behind a shock. A first order method will generally treat the same shock

correctly, but numerical diffusion will cause it to give low-resolution results in continuous parts of the flow.

We will be examining an alternative approach to computing discontinuous flows, known variously as Glimm's method, the Random Choice Method, or the Piecewise Sampling Method. This method was first used by Glimm [10] as part of a constructive existence proof of existence of solutions to systems of non-linear hyperbolic conservation laws. It was developed by Chorin [3,4] into an effective numerical method in the case of gas dynamics. In the first reference Chorin also introduced a multi-dimensional version of the scheme; in the second, he applied the method of reacting gas flow in one space variable. Since that time, the method had been used to compute compressible flow in cylindrical or spherical geometry (Sod [20,22]), and in applications to some problems in petroleum engineering (Concus and Proskurowski [7], Albright, Concus and Proskurowski [1], Glimm, Marchesin, and McBryan [10], Glimm, Marchesin, Isaacson, and McBryan [11]).

Although one computes solutions on a grid with Glimm's method, it is not a difference method. Rather than computing a weighted sum to arrive at the value of the solution at a grid point, one samples values from an explicit wave solution. Thus, the method has built into it an approximate form of wave transport and interaction, without the smoothing of such information inherent in averaging. The introduction of such a sampling technique as a numerical method is quite recent, compared to the length of time difference methods have been in use, and has not been subject to the extensive scrutiny and application from which the latter has benefitted. One of the purposes of this study is to indicate some of the features of Glimm's method which might make

developing it worth the effort, as well as a few of the directions in which the development might go.

We consider in this study two fundamental problems.

1)   We introduce a more accurate form of the sampling procedure for the one dimensional method than that used in [3], based on the van der Corput sampling sequence. We compare the performance of the van der Corput sampling and the previously used random sampling schemes.

2)   We investigate the operator splitting procedure by which Chorin constructs a multi-dimensional scheme from the one dimensional method. A source of error stemming from this procedure, not noticed in [3] is analyzed here and a method for eliminating it is proposed and tested.

In one-dimension, Glimm's method; with the appropriate sampling, is seen to be superior to any difference method in meeting the three criteria given above. The final method obtained for multidimensional calculations, although it does not share the special properties of the one dimensional method, has a number of interesting features, and is worthy of further investigation for its own sake.

This paper is divided into three sections. In Section 2 we discuss Glimm's method as applied to gas dynamics in one space variable. We define the van der Corput sampling sequences, and compare the van der Corput and random sampling strategies. In Section 3 we describe the operator splitting technique. In Section 4 we compare Glimm's method to some difference methods and give some conclusions, and suggestions for future work.

2. GAS DYNAMICS IN ONE SPACE VARIABLE

We want to construct approximate solutions to the initial value problem for Euler's equations for the motion of a one-dimensional, compressible, inviscid gas with a polytropic equation of state:

$$\frac{\partial U}{\partial t} + \frac{\partial F(U)}{\partial x} = 0$$

$$U(x,t) = U:R \times [0,T] \to R^3 \qquad\qquad (1.1)$$

$$U(x,0) = u(x) \quad \text{given}$$

$$U = \begin{pmatrix} \rho \\ m \\ E \end{pmatrix} \qquad\qquad F(U) = \begin{pmatrix} \rho \\ \frac{m^2}{\rho} + p \\ (E + p)\,\frac{m}{\rho} \end{pmatrix}$$

where ρ is the density, m is the momentum, and E is the total energy per unit volume of the gas. We can express in terms of these variables the more familiar quantities v the velocity, and ε, the internal energy of the gas:

$$v = \frac{m}{\rho} \qquad \varepsilon = \frac{E}{\rho} - \frac{u^2}{2} \qquad\qquad .$$

The pressure p which appears in the equation is a function of ρ, ε:

$$p = (\gamma - 1)\rho\varepsilon = A\rho^{\gamma}$$

where the constant $\gamma > 1$ is the ratio of specific heats for the gas. Another quantity of interest is the entropy, S, defined (up to an additive and a multiplicative constant)

$$S = \log (p\rho^{-\gamma}) = \log A$$

The system (1.1) is a first-order, hyperbolic system of conservation laws, i.e., the 3 x 3 matrix A(U) the Jacobian of F, has three real eigenvalues,

$$\lambda_1(U) = u - c, \quad \lambda_2(U) = u, \quad \lambda_3(U) = u + c$$

where

$$c = \sqrt{\frac{\gamma p}{\rho}}$$

is the adiabatic sound speed. λ_i, i = 1, 2, 3 are the characteristic velocities associated with the three modes of wave propagation for (1.1).

Since we are dealing with piecewise smooth solutions we interpret (1.1) in the sense of distributions. That is, if U(x,t) is discontinuous along a piecewise smooth curve $(\ell(t),t)$ then $d/dt = s(t)$ must satisfy

$$s(t)(U_L(\ell(t),t)) - U_R(\ell(t),t)) = F(U_L(\ell(t),t)) - F(U_R(\ell(t),t)) \tag{1.2}$$

where

$$U_{L,R}(\ell(t),t) = \lim_{\epsilon \uparrow 0, \epsilon \downarrow 0} U(\ell(t) + \epsilon, t)$$.

The discontinuity must also satisfy the entropy conditions (Courant and Friedrichs [8]). Discontinuities calculated using any of the numerical methods discussed in this paper satisfy the entropy conditions if they satisfy (1.2).

The simplest initial value problem for which discontinuities appear is one for which the initial data is constant on either side of the origin, where it has a jump discontinuity:

$$\phi(x) = \begin{cases} U_L & x < 0 \\ U_R & x > 0 \end{cases} \qquad U_L, U_R \in R^3$$

where we denote by

$$U_{L,R} = \begin{pmatrix} \rho_{L,R} \\ m_{L,R} \\ E_{L,R} \end{pmatrix} = \begin{pmatrix} \rho_{L,R} \\ \rho_{L,R} U_{L,R} \\ p_{L,R}/(\gamma - 1) + \tfrac{1}{2}\rho_{L,R}U^2_{L,R} \end{pmatrix}$$

This problem is known as the Riemann problem; its solution is a fundamental component of Glimm's method. The special case of the Riemann problem in which $U_L = U_R = 0$ is often referred to as the shock tube problem. The solution of the Riemann problem is discussed extensively in Chorin [3], Courant and Friedrichs [8], Godunov [12] and Sod [21] and van Leer. [23] In [3] and [21] detailed instructions for constructing solutions numerically are given; thus we will describe only qualitatively the structure of the solution.

Two general properties of the solution to a Riemann problem are that it is self-similar, i.e. $U(x,t) = h(x/t)$ for some piecewise continuous $h:R \to R^3$ and that it has the following additivity property: if $U(\xi,t\xi) = U_M \in R^3$ for some R then the function

$$U_1(x,t) \quad \begin{aligned} &= U(x,t) & \frac{x}{t} < \xi \\ \\ &= U_M & \frac{x}{t} > \xi \end{aligned}$$

is the solution to the Riemann problem with left and right states U_L, U_M. Similarly, the function

$$U_2(x,t) \quad \begin{aligned} &= U_M & \frac{x}{t} < \xi \\ \\ &= U(\chi,t) & \frac{x}{t} > \xi \end{aligned}$$

is the solution to the Riemann problem with left and right states U_M, U_R. Geometrically, this says that the solutions U_1, U_2 fit together to form U.

One can divide the (x,t) plane into four regions I, II, III, IV where $U(x,t)$ is constant (figure 1). These four regions are connected by three waves, each associated with one of the characteristic speeds. These are: a backwards facing sonic wave (associated with $u-c = \lambda_1(U)$, between $\ell_{1,b}$ and $\ell_{2,b}$; a contact discontinuity (associated with $u = \lambda_2(U)$, occurring across the line ℓ_s; and a forward facing sonic wave (associated with $u+c = \lambda_3(U)$ between $\ell_{1,f}$ and $\ell_{2,f}$. The pressure and velocity are continuous across

the line ℓ_s so they are equal to some fixed values p*, u* in II and III.

Only the density   changes across $\ell_s(t) = u*t$, from ρ_L^* to ρ_R^*.

As is discussed in [8], the hydrodynamic waves are uniquely determined by knowing the state of the gas on one side of the wave, and only the pressure on the other. For the backwards facing wave, for example, there are two possibilities. If p* > p_L then u* < u_L, $\rho_L^* > \rho_L$, $\ell_{1,b} = \ell_{2,b}$ and the wave is a shock associated with the characteristic velocity u-c. If p* < p_L, then we have a backwards facing centered rarefaction wave: $\ell_{1,b} < \ell_{2,b}$; p(x,t) and u(x,t) are continuous strictly monotone decreasing functions of x/t, and u(x,t) a continuous strictly monotone increasing function of x/t, for (x,t) between $\ell_{1,b}$ and $\ell_{2,b}$. The description of the forward facing wave is the same, replacing U_L by U_R, u by -u, and u+c by u-c.

In figure 2 we show the solution at a fixed time to the shock tube problem

$$P_L = 1.0 \qquad p_R = .1$$

$$P_L = 1.0 \qquad_R = 0.125 \qquad\qquad\qquad (1.3)$$

$$u_L = u_R = 0 \qquad \gamma = 1.4$$

The waves which occur are a backward facing rarefaction wave (A), a forward facing shock (B), and a contact discontinuity (C).

We can now describe Glimm's method for solving approximately the initial value problem (1.1). Let Δx be a spatial increment, Δt a time increment. We

assume that, at time $n\Delta t$, the approximate solution is constant on intervals of length Δx:

$$U^{(\Delta x)}(x, n\Delta t) = U_j^n \in R^3 \quad (j - \tfrac{1}{2})\, \Delta x < x < (j + \tfrac{1}{2})\, \Delta x \quad j = 0, \pm 1, \pm 2, \ldots \quad (1.4)$$

We wish to compute an approximate solution which at time has the same property:

$$U^{(\Delta x)}(x, (n + 1)\, \Delta t) = U_j^{n+1}$$

The procedure is given as follows:

1) Define $U_n^e(x,t)$ $n\Delta t < t < (n+1)\Delta t$ to be the exact solution to the initial value problem for (1.1) with initial data given by (1.4). The initial data consists of intervals where the solution is constant, separated by jump discontinuities; i.e., we have a succession of Riemann problems. If Δt is sufficiently small, then by finite propagation speed the waves from adjacent discontinuities do not intersect each other and the solutions to the adjacent Riemann problems fit together to given U_n^e (figure 3). A condition on Δt which guarantees that the waves do not intersect is

$$\frac{\Delta t}{\Delta x} = \lambda < \tfrac{1}{2} \qquad \sup_{\substack{x \, R \\ (n+1)\Delta t \,>\, t \,>\, n\Delta t}} |u_n^e(x,t)| + c_n^e(x,t)$$

When doing calcuations, one usually uses the more easily verified

$$\frac{\Delta t}{\Delta x} = \lambda < \sigma \sup_{x \in R} |u^{(\Delta x)}(x, n\Delta t)| + c^{(\Delta x)}(x, n\Delta t)$$

(1.4)

$$= \sigma \sup_{j} (|u_j^n| + c_j^n)$$

where σ is a constant, $0 < \sigma < \frac{1}{2}$

2)   Choose $a^{n+1} \in [0,1)$ and take

$$U_j^{n+1} = U_n^e \Big((j - \frac{1}{2} + a^{n+1}) \Delta x, \; (n + 1) \; \Delta t \Big)$$

(figure 4).

Thus we obtain a solution at time $(n+1)$ which depends on a sequence

$$\vec{a} = a^1, \; a^2, \; \dots;$$

much of the remainder of this section will be devoted to determining the best choice for the sequence a.

At first glance, this method might look complicated, but in fact it requires the evaluation of the solution to a Riemann problem once per zone per timestep. Let

$$h_{j-\frac{1}{2},n} \left(\frac{n - (j - \frac{1}{2})\Delta x}{t - n\Delta t} \right)$$

be the solution to the Riemann problem with left and right states U_{j-1}^n, U_j^n and let

$$\bar{U}_{j-\frac{1}{2}}^n = h_{j-\frac{1}{2},n} \left((a^{n+1} - \frac{1}{2}) \frac{\Delta x}{\Delta t} \right)$$

Then

$$U_j^{n+1} \quad \begin{aligned} &= \bar{U}_{j-\frac{1}{2}}^n \qquad a^{n+1} > \frac{1}{2} \\ &= \bar{U}_{j+\frac{1}{2}}^n \qquad a^{n+1} < \frac{1}{2} \end{aligned}$$

The procedure given here is slightly different from that used previously, in that the mesh is fixed, rather than shifting by $\Delta x/2$ every timestep. By sampling back to a fixed grid, the relation to Godunov's method is immediate: in Godunov's method, U_j^{n+1} is taken to be

$$\frac{1}{\Delta x} \int_{(j - \frac{1}{2})\Delta x}^{(j + \frac{1}{2})\Delta x} U_n^e(x, \Delta t)\, dx \qquad ;$$

in Glimm's method, one chooses a representative point value of the local exact solution.

The mechanism by which Glimm's method models wave propagation in a gas is most easily demonstrated by the following example. Let U_L, U_R be the left and right states of a Riemann problem whose solution consists of a single discontinuity propagating at speed $s > 0$. The exact solution for this problem is

$$U(x,t) \quad \begin{array}{ll} = U_L & x < sT \\ = U_R & x > sT \end{array}$$

We will solve this initial value problem using Glimm's method. First, it is obvious that, for any time step n there is an

$$\ell(n) = j_0 - \tfrac{1}{2},$$

j_0 an integer, such that

$$U_j^n \quad \begin{array}{ll} = U_L & j < \ell(n) \\ = U_R & j > \ell(n) \end{array}$$

$\ell(n)$ is the location of the shock in the approximate solution, and satisfies

$$\ell(n+1) \quad \begin{array}{llll} = \ell(n) & \text{if} & a^{n+1} > \lambda s \\ = \ell(n + 1) & \text{if} & a^{n+1} < \lambda s \end{array}$$

$$\ell(0) = \tfrac{1}{2}$$

So that

$$\ell(n) = \ell(0) + N \left\{ j = 1, \ldots, n; \ a^j \in 0, \lambda s) \right\}$$

where

$$N\{ j = n_1 + 1, \ \ldots, \ n_2, \ a^j \in I \}$$

denotes the number of j, $n_1 < j \le n_2$ such that a^j is contained in I. We say that a sequence a is equidistributed if the proportion of times that a^j is contained in I is asympotically equal to $|I|$, the length of I, i.e., if we define

$$\frac{1}{n_2 - n_1} N\{ j = n_1 + 1, \ \ldots, \ n_2; \ a_j \ I \} - |I| \equiv \delta(\vec{a}, n_1, n_2, I)$$

then a is equidistributed if $\lim \ \delta(\vec{a}, n_1, n_2, I) = 0$ for each fixed n_1,

$$n_2 \to \infty,$$

I. Given this notation we write

$$\ell(n)\Delta x = \ell(0)\Delta x + \Delta x \lambda s n + \delta(\vec{a}, 0, n, \ 0, \lambda s)) \ n\Delta x$$

$$= \ell(0)\Delta x + n\Delta t (1 + \frac{1}{\lambda} \delta \ a, 0, n, (0, \lambda s))$$

If a is equidistributed, then

$$\ell(n) \ \to \ sT \qquad \qquad \text{in the limit } n \to \infty \quad ,$$

$$|n\Delta t - T| < \Delta t \ , \ \frac{\Delta t}{\Delta x} = \lambda > 0$$

Thus the shock in the approximate solution at each time step either moves by Δx or does not move at all. Over many time steps, the cumulative displacement is close to that of the exact solution, the leading term in the error being proportional to $\delta(\vec{a}, 0, n, [0, \lambda s))$. In general, a piecewise continuous flow will be represented by $O(1/\Delta x)$ waves of strength $O(\Delta x)$, all having differing speeds, as well as an $O(1)$ number of discontinuities of strength $O(1)$. Furthermore, the speeds and strengths of the waves will be changing in a piecewise continuous fashion as a function of time. In order to model such a flow correctly by the above mechanism, one needs to choose $\vec{a}$ such that δ is small as possible, uniformly in $\dot{I}$, n_1 for n_2-n_1 large relative to 1, but $(n_2-n_1)\Delta t$ small relative to the characteristic times in which the wave speeds change. The sampling procedure given below seems to be optimal from the point of view of these requirements.

The simplest form of this sampling sequence is due to van der Corput (see [14]). Let

$$n = \sum_{k=0}^{m} i_k 2^k \quad i_k = 0, 1 \quad \text{be the binary expansion of } n = 1, 2, \ldots$$

Then $a^n = \displaystyle\sum_{k=0}^{m} i_k 2^{-(k+1)}$

The easiest way to see how the sequence is constructed is to write down the first few elements in it:

$$1 = 1_2 \qquad a^1 = .5 \qquad = .1_2$$

$$2 = 10_2 \qquad a^2 = .25 \qquad = .01_2$$

$$3 = 11_2 \qquad a^3 = .75 \qquad = .11_2$$

$$4 = 100_2 \qquad a^4 = .125 \qquad = .001_2$$

$$5 = 101_2 \qquad a^5 = .625 \qquad = .101_2$$

$$6 = 110_2 \qquad a^6 = .375 \qquad = .011_2$$

$$7 = 111_2 \qquad a^7 = .875 \qquad = .111_2$$

$$8 = 1000_2 \qquad a^8 = .0625 \qquad = .0001_2$$

So $a_i \lesssim .5$ if i is $\begin{matrix} \text{even} \\ \text{odd} \end{matrix}$; $\frac{k}{4} \le a^i < \frac{k+1}{4}$ if i $\quad$ j(k) mod 4,

k = 0, 1, 2, 3 where j(0) = 0, j(1) = 2, j(2) = 1, j(3) = 3. In general, if

one divides the unit interval into the subintervals

$$(r2^{-S}, (r + 1) 2^{-S}) \quad r = 0, \ldots, 2^S - 1 \quad,$$

then for each r there is exactly one q for which $q_0 < q < q_0 + 2^S$ such

that $a^q \in [r2^{-S}, (r+1)2^{-S})$.

We will have need of a variant of this procedure for use in multi-

dimensional problems. Let k_1, $k_2 > 0$ be integers, $k_1 > k_2$ relatively

prime. The (k_1, k_2) van der Corput sampling sequence $\vec{a}$ is given by

$$a^n = \sum_{\ell=0}^{m} q_\ell \cdot k_1^{-(\ell + 1)}$$

where

$$q_\ell \equiv k_2 i_\ell \bmod k_1, \quad \text{and} \quad \sum_{\ell = 0}^{m} i_\ell k_1^\ell = n$$

is the base k_1 expansion of n. Thus the binary van der Corput sampling sequence given above is the special case $k_1 = 2$, $k_2 = 1$.

All the van der Corput sampling sequences are equidistributed. In fact

$$\delta(a, n_1, n_2, I) \leq (C_1 \log k_1 (n_2 - n_1) + C_2)/(n_2 - n_1)$$

where C_1, C_2 are constants depending on k_1, k_2 but not on n_1, n_2 or I. For the binary van der Corput sequence $C_1 = 3$, $C_2 = 1$. In the example given above, this gives an error bound of $O(\Delta x | \log \Delta x |)$

In previous computational work for gas dynamics using Glimm's method, random sampling was used, i.e. the were drawn from a random number generator implemented on the computer, usually with some variance reduction technique, such as stratification for random sampling, for which

$$\delta = O\left(\frac{1}{\sqrt{n}}\right)$$

giving an error bound in our simple shock example of $O(\sqrt{\Delta x})$.

Lax [17] proposed the use of a non-random equidistributed sequence due to Richtmeyer and Ostrowski, defined by $a^n \equiv n \sqrt{r} \bmod 1$ where r is an integer which is not the square of another integer.

We shall not discuss the Richtmeyer-Ostrowski sampling sequence in detail here, save to note that in numerical experiments, and in simple analytical examples, one obtains results using the Richtmyer-Ostrowski sequence similar

to those obtained using van der Corput sampling. However, the bound on δ is stronger for the van der Corput sequence than that obtained for the Richtmyer-Ostrowski sequence, as well as being explicitly uniform in I and n_1; uniformity in I and n_1, does not hold explicitly for the Richtmyer-Ostrowski sequence. Also, Van der Corput sampling has some special properties which guarantee that certain qualitative features of the continuous part of the solution preserved in the approximate solution, at least for simple waves (see [5], [6]). Finally, van der Corput sampling has several straightforward extensions to two or more dimensions which guarantee good distribution properties in the square, even for finite sample sizes. In contrast, it has been pointed out by Maltz and Hitzl [18] that such an extension of the Richtmyer-Ostrowski sequence can give rise to poor distribution in the square for finite sample sizes due to resonance effects.

In an effort to understand the errors introduced by the interaction of the sampling and variations in time in the wave speeds, we consider the following class of test problems. The initial data consists of two discontinuties located at x , and x_r, separated by constant states:

$$
U(\chi,0) \quad
\begin{aligned}
&= U_\ell & x &< x_\ell \\
&= U_m & x_\ell &< x < x_r \\
&= U_r & x &> x_r
\end{aligned}
$$

$$
U_{\ell,m,r} = \begin{pmatrix} \rho_{\ell,m,r} \\[1em] \rho_{\ell,m,r} u_{\ell,m,r} \\[1em] \dfrac{p_{\ell,m,r}}{(\gamma - 1)} + \tfrac{1}{2}\, \rho_{\ell,m,r}\, u^2_{\ell,m,r} \end{pmatrix}
$$

We choose U_ℓ, U_m, U_r such that U_ℓ and U_m can be connected by a forward-facing shock and that U_m and U_r can be connected by a forward-facing centered rarefaction wave (figure 5).

The shock overtakes the rarefaction, the cancellation between them weakening both (figure 6,(A)). The nonlinear coupling between the modes produces waves of the other two families in back of the shock and moving to the left, away from the shock. These are, a backwards facing compression wave (figure 6, (B)), and a strong entropy/density wave (figure 6, (C)) advected passively by the velocity field $u(x,t)$.

In figures 7-9 we show the calculation of such a problem using Glimm's method with, respectively, a random sampling sequence, a stratified random sampling, and the binary van der Corput sampling sequence. The initial data are:

$$\rho_\ell = 26.869 \qquad \rho_m = 1.39 \qquad \rho_r = 10.$$

$$\rho_\ell = .6878 \qquad \rho_m = .146 \qquad \rho_r = .6$$

$$u_\ell = .0181 \qquad u_m = -11.9 \qquad u_r = -5.98$$

$$x_\ell = .4 \qquad x_r = .9 \qquad \gamma = 1.4$$

All calculations were done on the spatial interval [0,1] with boundary conditions at 0 and 1 obtained by assuming the solutions satisfy

$$\left.\frac{\partial U}{\partial x}\right|_{x=0,1} = 0 \qquad .$$

The various solutions being compared were computed with $\Delta x = .01$ and are represented graphically by circles for the computed values at mesh points, interpolated by a dotted line. Also plotted on each of the graphs with a solid line, is a solution obtained using Glimm's method, with van der Corput and $\Delta x = .0025$. Having compared the latter solution with a similar one done for $\Delta x = .005$ we found that the two results differed by less than .5%, so that the method has converged for $\Delta x = .0025$. For the purposes of comparing the various $\Delta x = .01$ solutions, we treat the $\Delta x = .0025$ solutions as exact, against which the $\Delta x = .01$ solutions can be compared.

The sampling governs the rate at which the shock and rarefaction interact. If $s_{q+\frac{1}{2}}^n$ is the speed of the shock, located between zones q and q + 1 at time step n, and $\lambda_+^n = u_{q+1}^n + c_{q+1}^n$, then the shock will cancel with a piece of the rarefraction wave, and produce more wave of the other two families, at time step n + 1 if and only if $a^{n+1} \in \left[\frac{\Delta t}{\Delta x} \max(\lambda_+^n, 0), \frac{\Delta t}{\Delta x} s_{q+\frac{1}{2}}^n \right)$. Thus the loss of gradient information observed in the randomly sampled solution (figure 7) is a result of random fluctuations in the rate of interaction between the shock and rarefaction which is producing the wave. The use of stratified random sampling (figure 8) produces smoother profiles than those obtained with the unmodified random sequence, but the shape of the entropy wave is incorrect; in particular, there is a sizable deviation in the density profile, a failure to conserve mass. The profile obtained using van der Corput sampling (figure 9) is in much closer agreement with the $\Delta x = .0025$

result, the rate of wave production being modeled much better than in the other two cases. In fact, if one uses van der Corput sampling, one can use a much coarser mesh and still get good results for this problem. In figure 10 we present the results obtained on this problem with binary van der Corput sampling, and Δx = 1/30. The absolute locations of the waves, and their locations relative to each other, are correct to within Δx; more important, the size and shape of the waves, which are more sensitive to the cumulative error introduced by the sampling, are in very close agreement with the Δx = .0025 result. In all the calculations, the shock discontinuity is sharp, as guaranteed by Glimm's method.

3. Operator Splitting

In [3], Chorin proposed a method for computing multi-dimensional unsteady compressible flow using Glimm's method by means of operator splitting. We can write the equations of motion for an ideal gas in two space dimensions as

$$\frac{\partial U}{\partial t} + \frac{\partial}{\partial x}(F(U)) + \frac{\partial}{\partial y}(G(U)) = 0$$

$$U(x,y,t) = U:R^2 \times [0,T] \to R^4$$

$$U(x,y,0) = \phi(x,y) \quad \phi:R^2 \to R^4$$

$$U = \begin{pmatrix} \rho \\ m \\ n \\ E \end{pmatrix}, \quad F(U) = \begin{pmatrix} m \\ \frac{m^2}{\rho} + p \\ \frac{mn}{\rho} \\ \frac{m}{\rho}(E+p) \end{pmatrix}, \quad G(U) = \begin{pmatrix} n \\ \frac{mn}{\rho} \\ \frac{n^2}{\rho} + p \\ \frac{n}{\rho}(E+p) \end{pmatrix}$$

Here ρ is the density, m is the x-component of momentum, n is the y-component of momentum, and E is the total energy. We can express the velocity $\vec{v}$ and the internal energy ϵ in terms of the above variables: $v_x = \frac{m}{\rho}$ is the x-compondent of the velocity, $v_y = \frac{n}{\rho}$ is the y-component of the velocity, and $\epsilon = \frac{E}{\rho} - \frac{1}{2}(v_x^2 + v_y^2)$. The pressure p is a function of ρ and ϵ: $p = (\gamma - 1)\rho\epsilon$ where γ, the ratio of specific heats, is a constant assumed to be greater than 1. Thus, as was the case for one space variable, the value U at a given point is uniquely determined by the values of ρ, p and $\vec{v}$ at that point.

We wish to construct approximate solutions

$$U^{\Delta x, \Delta y}(x,y,n\Delta t) = U^n_{i,j} \in R^4$$

$$(i - \tfrac{1}{2})\Delta x < x < (i + \tfrac{1}{2})\,\Delta x$$

$$(j - \tfrac{1}{2})\Delta y < y < (j + \tfrac{1}{2})\,\Delta y$$

where x, y are spatial increments, t is a time increment, and i,j,n are integers, $n \geq 0$.

Assume we know $U^n_{i,j}$ and want to find $U^{n+1}_{i,j}$; the procedure is as follows:

1) For each j perform one time step of Glimm's method for the equation

$$\frac{\partial V}{\partial t} + \frac{\partial}{\partial x}(F(V)) = 0 \qquad ,$$

taking as initial data $V^0_i = U^n_{i,j}$. Set the results $V^1_i = U^{n+\frac{1}{2}}_{i,j}$
(we denote this procedure by $(L^x_{\Delta t}U^n)_{i,j} = U^{n+\frac{1}{2}}_{i,j}$,

2) For each fixed i perform one time step of Glimm's method for the equations

$$\frac{\partial V}{\partial t} + \frac{\partial}{\partial y}(G(V)) = 0 \qquad ,$$

taking as initial data $V_j^0 = U_{i,j}^{n+\frac{1}{2}}$, time step t. Set the result $V^1 = U_{i,}^{n+1}$ (we denote this procedure by

$$\left(L_{\Delta t}^y U^{n+\frac{1}{2}}\right)_{i,j} = U_{i,j}^{n+1}$$

The solution thus derived at time $(n+1)\Delta t$ is interpreted as being the piecewise constant function

$$U^{\Delta x, \Delta y}(x, y, (n+1)\Delta t) = U_{i,j}^{n+1}$$

$$(i - \tfrac{1}{2})\Delta x < x < (i + \tfrac{1}{2})\Delta x$$

$$(j - \tfrac{1}{2})\Delta y < y < (j + \tfrac{1}{2})\Delta y$$

A necessary condition on the time step t is that it must satisfy (1.4) for each of the one-dimensional calculations:

$$\frac{\Delta t}{\Delta x} < \sigma \max_{i,j} \left(|v_{x,i,j}^n| + c_{i,j}^n \right)$$

$$\frac{\Delta t}{\Delta y} < \sigma \max_{i,j} \left(|v_{y,i,j}^n| + c_{i,j}^n \right), \quad 0 < \sigma < \tfrac{1}{2}$$

(3.1)

The above procedure is formally the same as is done to construct multi-dimensional difference methods from one-dimensional ones. However, the mechanism by which Glimm's method propagates the solution to the equation in one dimension is rather different than that of difference methods, as it

requires many time steps for the cumulative effect of the sampling to give the correct wave speeds; therefore the actual justification of the splitting procedure, currently unknown, is likely to be quite different than the usual truncation error analysis for difference methods.

The Riemann problems in question are easily solved, given the solution for one-dimensional gas dynamics. For example, to solve Riemann's problem for

$$\frac{\partial V}{\partial t} + \frac{\partial}{\partial x} (F(V)) = 0$$

$$V = (\bar{\rho}, \bar{\rho}\bar{v}_x, \bar{\rho}\bar{v}_y, \frac{\bar{p}}{\gamma - 1} + (\bar{v}_x^2 + \bar{v}_y^2) \frac{\bar{\rho}}{2})$$

take the solution $\rho(x,t)$, $p(x,t)$, $u(x,t)$ in Section 2 with

$$\rho_{L,R} = \rho_{L,R}, \ p_{L,R} = p_{L,R}, u_L = v_{x,L}, \ u_R = v_{x,R}$$

$$\rho(x,t) = p(x,t), \ p(x,t) = p(x,t), \ v_x(x,t) = u(x,t) \qquad ;$$

$$v_y(x,t) = v_{y,L}$$

if (x,t) is to the left of the contact discontinuity ℓ_s

$$v_y(x,t) = v_{y,R}$$

if (x,t) is to the right of the contact discontinuity ℓ_s. Thus in the x-sweep, we have ordinary 1-D gas dynamics, with the discontinuity in v_y passively advected. To solve the Riemann problem for

$$\frac{\partial V}{\partial t} + \frac{\partial}{\partial y} \left(G(V) \right) = 0 \qquad ,$$

interchange the roles of v_x and v_y.

To test the validity of this procedure, we looked at the simplest two-dimensional test problem possible. We took our computational domain to be the unit square with the computational mesh aligned with the x- and y-axes, and took the initial conditions to be

$$U(x,y) \quad \begin{matrix} = U_R & x < y \\[1em] = U_L & x > y \end{matrix}$$

$$U_L = \begin{pmatrix} \rho_L \\ \rho_L v_{x,L} \\ \rho_L v_{y,L} \\ p_L/(\gamma-1) + \frac{\rho_L}{2} (v_{x,L}^2 + v_{y,L}^2) \end{pmatrix} \qquad U_R = \begin{pmatrix} \rho_R \\ \rho_R v_{x,R} \\ \rho_R v_{y,R} \\ p_R/(\gamma-1) + \frac{\rho_R}{2} (v_{x,R}^2 + v_{y,R}^2) \end{pmatrix}$$

This is the Riemann problem, for which we have an analytic solution. Computationally, it is a two-dimensional problem, since the initial discontinuity is at a 45° angle to the mesh directions.

We denote by v_n the component of the velocity normal to $x = y$, v_t the component parallel to $x = y$.

$$v_n = \frac{v_x - v_y}{\sqrt{2}} \qquad\qquad\qquad v_t = \frac{v_x + v_y}{\sqrt{2}}$$

$$v_{n,R} = \frac{v_{x,R} - v_{y,R}}{\sqrt{2}} \qquad\qquad v_{t,R} = \frac{v_{x,R} + v_{y,R}}{\sqrt{2}}$$

$$v_{n,L} = \frac{v_{x,L} - v_{y,L}}{\sqrt{2}} \qquad\qquad v_{t,L} = \frac{v_{x,L} + v_{y,L}}{\sqrt{2}}$$

Throughout these test calculations we will set $v_{t,L} = v_{t,R} = 0$, i.e., we will be looking at problems for which there is no slip line in the exact solution. Unless otherwise indicated, the calculations shown were done on a 50x50 grid: $\Delta x = \Delta y = .02$. The results of the calculations are displayed by plotting the profiles of various quantities along the line $y = 1 - x$, and comparing them with the exact solution. In these plots, the computed values at the mesh points are graphed as circles, interpolated by a dotted line: the exact solution is plotted as a solid line. When boundary conditions are required, we assume the solution is constant on lines parallel to the initial jump. This was quite effective in preserving the symmetry of the solution, and enabled us to run for long times without noise from the boundary affecting the results.

The one-dimensional calculations using Glimm's method in the x and y directions require sampling sequences $\vec{a}_x$, $\vec{a}_y$ which we took to be two independent van der Corput sampling sequences: $\vec{a}_x$ was the (3,2) van der Corput sequence, and $\vec{a}_y$ was the (5,3) van der Corput sequence. This insured optimal distribution in the square $[0,1) \times [0,1)$.

In figure 11, we show the results for the following problem:

$$\rho_L = .353 \qquad\qquad \rho_R = .1$$

$$p_L = 14.0 \qquad\qquad p_R = .5 \qquad\qquad\qquad (3.2)$$

$$v_{N,L} = -1.78 \qquad\qquad v_{N,R} = 11.6 \qquad\qquad \gamma = 1.667$$

The exact solution is a strong, right-facing shock. It is almost stagnant (after 175 time steps, the exact shock point has moved only two zones). By this time, the oscillations (80% of the exact post-shock value in the pressure) have begun to make themselves known by a three zone error in the shock location, the shock moving a distance more than two times greater than it should have. We see substantial values (60% of $|v_{n,L} - v_{n,R}|$) for v_T (x,y,t) the tangential component of the velocity appearing. Finally, the density profile shows a substantial deviation from conservation of mass.

The fundamental reason why large errors occur in this problem is that, although each half-step $L^x_{\Delta t}$, $L^y_{\Delta t}$ models the resulting one-dimensional gas dynamics well, the problem it is modeling is O(1) incorrect from the point of view of the two-dimensional flow. For example, consider the problem one solves (one for each value of j) in the first x-pass in the test problem 3.1. They are each the same Riemann problem for a one-dimensional gas flow, with the jump taking place along the diagonal. The left and right states

$$V_{L,R} = \begin{pmatrix} \bar{\rho}_{L,R} \\[2mm] \bar{\rho}_{L,R}\, \bar{U}_{L,R} \\[2mm] \bar{\rho}_{L,R}(\bar{v}_y)_{L,R} \\[2mm] \dfrac{\bar{p}_{L,R}}{\gamma-1} + (\bar{u}^2_{L,R} + (\bar{v}^2_y)_{L,R})\,\dfrac{\bar{\rho}_{L,R}}{2} \end{pmatrix}$$

for the one-dimensional problem are

$$\bar{p}_{L,R} = p_{L,R} \qquad\qquad\qquad \bar{\rho}_{L,R} = \rho_{L,R}$$

$$\bar{u}_L = \frac{v_{n,L}}{\sqrt{2}} \qquad \bar{u}_R = \frac{v_{n,R}}{\sqrt{2}} \qquad v_{y,L} = \frac{v_{n,L}}{\sqrt{2}} \qquad v_{y,R} = \frac{v_{n,R}}{\sqrt{2}}$$

The jump in the velocity, $u_L - u_R$, is less than $v_{n,L} - v_{n,R}$ so a weaker forward-facing shock than that of the original two-dimensional problem is produced, as well as a backwards-facing rarefaction wave. If we sample anywhere in the fan other than the left or right states, we get a

$$(v_x)^{n+\frac{1}{2}}_{i,j} > u_L, u_R \qquad .$$

The new values

$$(v_x)^{n+\frac{1}{2}}_{i,j} \,,\; \rho^{n+\frac{1}{2}}_{i,j} \,,\; p^{n+\frac{1}{2}}_{i,j}$$

depend only on the sampling value a_x^1 and the ratio $\Delta t/\Delta x$ but not on Δt and Δx separately. So the difference between these and the exact answer is an $O(1)$ quantity relative to the mesh spacing. In particular, there is an $O(1)$ contribution to the tangential component of the velocity. Since there has been an $O(1)$ change in the thermodynamic variables p and ρ, there is no reason for the y-pass to produce a tangential velocity to cancel the one produced by the x-pass, and in fact it does not. Similar phenomena occur for a shock tube, (figure 12) or a Riemann problem whose solution consists of two centered rarefaction waves.

The above failures in the splitting procedure in situations when there are discontinuties in $p,\vec{v}$ can be viewed as a consequence of an invalid interchange of limiting procedures. Analytically, shock solutions are obtained as limits of viscous solutions as some set of diffusion coefficients go to zero. One might try to obtain the shocked solutions by using an operator splitting method to solve the viscous equations; the splitting procedure is then known to converge as $\Delta t \to 0$. Then, in the inviscid limit, the viscous solutions converge to the physically correct shocked solutions. In a difference method, the two limiting procedures take place simultaneously, with the coefficients multiplying the numerical diffusion approaching zero with Δt. The use of operator splitting with Glimm's method corresponds to letting the diffusion coefficients vanish for nonzero Δt. This interchange of limits is valid for continuous solutions, or near contact discontinuities, but near discontinuities in p or $\vec{v}$ the two limiting procedures are singular with respect to each other, and cannot be interchanged freely.

In order to correct this problem, we replace Glimm's method at discontinuities in p and $\vec{v}$ with a conservative finite difference method; the method we use in the nonlinear Godunov method (Godunov [2], Richtmyer and Morton [19]) adapted for Eulerian coordinates (Godunov, et al [13]).

We describe the procedure for advancing this hybrid Glimm-Godunov method by one timestep, in one space dimension; the extension to two space dimensions, is achieved by an operator splitting procedure like the one described above. First, one calculates the exact solution to the initial value problem to (1.1), as before. At those mesh points where one uses Glimm's method, one samples as before. At those mesh points $(j\Delta x, (n+1) \Delta t)$ where one wishes to use Godunov's method, one sets

$$U_j^{n+1}{}_{Godunov} = \frac{1}{\Delta x} \int_{(j - \frac{1}{2})\Delta x}^{(j + \frac{1}{2})\Delta x} U^e(x, (n + 1) \Delta t) \, dx$$

By integrating the conservation law over the rectangle $[(j - \frac{1}{2})\Delta x, (j + \frac{1}{2}) \Delta x] \times [n\Delta t, (n + 1) \Delta t]$ we obtain, using the notation of Sec. 2,

$$U_j^{n+1}{}_{Godunov} = U_j^n + (F(h_{j-\frac{1}{2}, n}(0)) - F(h_{j+\frac{1}{2}, n}(0))) \frac{\Delta t}{\Delta x}$$

where F is the vector of fluxes for the conservation law being integrated. Finally, we need a perscription for deciding whether to use Glimm or Godunov. Let

$$p_j^{max} = \max \ (p_j^n, p_{j-\frac{1}{2}}^{n*})$$

$$- \ k_0 \leq k-j \leq k_0 + 1$$

$$p_j^{min} = \min \ (p_j^n, \ p_{j-\frac{1}{2}}^{n*})$$

$$- \ k_0 \leq k-j \leq k_0 + 1$$

where $p_{j-\frac{1}{2}}^{n*}$ is the pressure in the region separating the two sonic waves which come from the Riemann problem centered at $((j-\frac{1}{2})\Delta x, n\Delta t)$ (see [3], [21]; and the appendix to this paper). Then the perscription for choosing Glimm and Godunov is

$$(U_j^{n+1})_{hybrid} \quad \begin{array}{l} = (U_j^{n+1}) \ \text{Godunov} \\ \\ = (U_j^{n+1})_{Glimm} \end{array} \quad \begin{array}{l} \text{if} \quad \dfrac{p_j^{max} - p_j^{min}}{p_j^{min}} \ > \ c_0 \\ \\ \text{otherwise} \end{array}$$

Here c_0, k_0 are constants to be set at the beginning of the calculation. Roughly, c_0 is a measure of the strength of the weakest sonic wave in the problem that must be treated as a discontinuity, and $k_0 + 1$ is the effective width of a discontinuity. For weak problems (excess pressure ratios ≤ 5), it suffices to set $k_0 = 1$. For stronger shocks, it appears to be necessary to set $k_0 = 2$. In all the calculations presented here, $.05 \leq c_0 \leq .2$. The consequence of the nonoptimal choice of parameters is a loss of accuracy, not of stability: failing to detect a pressure jump results in noise; using Godunov's method unnecessarily results in the smoothing of relevant wave structures.

One can make several minor modifications of the method described above. The fact that we are using Godunov's method near strong pressure jumps makes it possible to introduce some approximations into the solution of the Riemann problem. Another consequence of sampling only if the sonic waves are weak is that, by accounting approximately for the interaction of those waves, one can use a larger time step, allowing $\sigma < 1$ in 3.1, which is the time step restriction for Godunov's method. We have implemented both of these changes in the method for the examples computed here; in an appendix to this paper, we describe the details of the algorithms used. Finally, we noticed that the first order splitting algorithm described above can lead to errors near very strong shocks (excess pressure ratios greater than 100) computed using Godunov's method. In particular, large tangential components of velocity are generated behind the shock. We found that the use of the Strang splitting algorithm

$$U^{n+2} = L^x_{\Delta t} L^y_{\Delta t} L^y_{\Delta t} L^x_{\Delta t} U^n$$

reduced this error to the level found in regions where the flow is continuous.

In figure 13, we show the results for the problem 3.2 using the hybrid method. Since the solution is a shock discontinuity separating two constant states, this calculation is mostly a test of how well the nonlinear Godunov's method computes a strong shock. The dip in the density behind the shock is a starting error, common to most conservative difference methods; it comes from starting a strong shock as a jump discontinuity. Since there is no numerical viscosity away from the shock the oscillation is not damped, but flows downstream unchanged.

Figure 14 shows the results obtained for the shock tube problem 1.3 calculated as a diagonal Riemann problem; figure 15 shows the result for the same problem using Godunov's method alone. The hybrid method treats the shock correctly, as opposed to the Glimm's method alone (figure 12). The hybrid method is also an improvement over Godunov's method alone: the three waves are clearly resolved; in particular, the contact discontinuity is spread over only three zones. We have found that, in general, the hybrid method spreads any discontinuity over a small (1-4) number of zones, independent of the zone size, regardless of whether the discontinuity is a shock, contact discontinuity, or slip surface.

In order to test this method on a more complex problem, we computed a two-dimensional Cartesian shock reflection problem used by van Leer [23] as a test problem; Woodward [24] has compiled a comparison of various difference methods, based on this problem. The computational domain is a channel of unit length, open at both ends. For x < .2, the channel has width 1/3; at x = .2, the lower side of the channel is constricted, so that the width of the channel is 4/15 for x > .2. Reflecting boundary conditions are imposed on the upper and lower sides of the channel, and on the segment x = .2, $0 \le y \le 1/15$. The solution is assumed to be continuous at both ends. The initial conditions for this problem are those of uniform flow throughout the tube:

$$p(x,y,0) = 1. \quad \rho(x,y,0) = 1.4. \quad v_x(x,y,0) = 3. \quad v_y(x,y,0) = 0. \quad \gamma = 1.4$$

with these initial conditions, a detached shock reflects off the constriction, and reflects off the upper side of the channel, having formed by time t = 4/3

a three-shock Mach reflection configuration. According to Woodward [24], the correct location of the Mach stem along the side of the channel is right above the constriction at x = .2; the Mach stem should extend about one-fourth the distance across the left end of the channel.

We show results obtained using Godunov's method by itself (figure 16), and the hybrid method, with two different zone sizes (figures 17,18). The solution obtained using Godunov's method alone has the shock slightly in back of the step with the Mach stem about half the correct length. The slip line emerging to the right of the triple point is spread over four or more zones, except right at the shock. The solutions obtained with the hybrid method both have the shock in the correct position to within one zone length, and the length of the stem differs from the correct length by two zone lengths. Both of the hybrid calculations have the slip line spread across two zones for its entire length.

4. Discussion and Conclusions

In one space variable, Glimm's method has built into it an approximate form of linear and nonlinear wave propagation along characteristics, without the smoothing of such information, as occurs in difference methods, and without any complicated bookkeeping; the sampling procedure determining the weakest wave or wave interaction to be resolved. The motivation for using van der Corput sampling is that one obtains the best possible representation of the wave propagation in Glimm's method, independent of the speed of the waves. This is essential for the correct representation of continuous waves, particularly those produced by nonlinear wave interactions.

We would like to compare the performance of Glimm's method to that of difference methods. Sod [21] performed such a comparison, using a one dimensional shock tube problem. The results obtained there were not the best possible, due to the use of stratified random sampling. On the other hand, comparing difference methods to Glimm's method on this problem is not entirely fair either. As is pointed out in [4], it follows from the additivity property for solutions to the Riemann problem that the only values taken on by the computed solution are ones taken on by the exact solution as well. In any case, we present in figure 19 the calculation done with Glimm's method, but using van der Corput sampling. The result obtained here is clearly superior to any of those in [21].

We compared the performance of Glimm's method to that of two difference methods on a shock and rarefaction interaction problem (figure 20) like the one described in Sec. 3, but with the waves an order of magnitude stronger:

$p = 473.9$ $p_m = 1.077$ $p_r = 100.$

$p_\ell = 23.27$ $\rho_m = 3.930$ $\rho_r = 100.$

$u = 6.0$ $u_m = -4.0$ $u_r = -1.181$

$x_\ell = .3$ $x_r = .9$ $= 1.4$

The solution has the same qualitative features as those of the weaker problem; except that the backwards-facing compression wave produced by the shock-rarefaction interaction has itself steepened into a shock at the time the solutions are compared. Otherwise, the waves are all much stronger; in particular, the passively advected density wave is a spike, two zones in width for the $x = .01$ cases. The two difference methods compared are the version of Godunov's method (figure 21) discussed in the previous section, and the MUSCL code written by Paul Woodward of LLNL, based on the scheme of van Leer 23 (figure 22). These two methods represent, respectively, one of the most accurate of the first-order methods, and a state of the art representative of the adaptive or hybrid difference methods (for other examples see Boris and Book [2], Harten [15], Harten and Zwas [16], Zalesak [25]). As before, we compare all three results with the answer obtained using Glimm's method, van der Corput sampling with $\Delta x = .0025$. All three methods obtain reasonably good answers for the pressure and velocity profiles, modulo the varying widths for the shock transition region. However, neither of the difference methods are

able to get the correct peak value of the density, nor the correct width for the density spike; Glimm's method, by virtue of its direct simulation of the wave interaction process without averaging, gets the correct answer.

The original proposal in [3] for using Glimm's method with operator splitting was seen to give incorrect results for flows in which there occur large jumps in the pressure and velocity along surfaces oblique to the mesh directions. By coupling Glimm's method with Godunov's method, we lose many of the special properties of the Glimm's method with respect to its treatment of shock interactions. However, the resulting method has a number of attractive properties. Of all the first-order difference methods, Godunov's method produces the narrowest shocks (2-3 zones wide). Both Glimm's method and Godunov's method are extremely stable, even in the strongly nonlinear region (the problem with Glimm's method at shocks is a loss of accuracy, not of stability). Finally, Glimm's method has no numerical diffusion, so that the hybrid method has no numerical diffusion away from regions where large pressure gradients are generated.

For the purpose of comparison with the results of Sod [21], obtained by the various difference methods, we computed the shock tube problem 1.3 as a diagonal Riemann problem, (figure 23), but on a 100 x 100 grid ($\Delta x = \Delta y = .01$); results for this problem compted using the MUSCL code are also given in [23]. In principle, the problem solved here is more difficult than the one solved in [21], since in the latter it is solved as a one-dimensional problem. But the answer is the same for both, and the results are worth comparing.

The calculation of the rarefraction, and the width of the shock transition in the results obtained with the hybrid Glimm-Godunov method compare favorably with those obtained by any of the difference methods. The treatment of the contact discontinuity is clearly superior to that given by any of the difference methods in [21], and comparable to that obtained in [23]. The difference methods in [21] either spread the contact discontinuity over 6-10 zones, with the number of zones increasing as a function of time, or introduce substantial oscillations near the contact discontinuity.

The major weakness of the hybrid method is that it computes shocks which are 2-3 zones wide. This puts the method at a disadvantage to the methods which have narrower shocks in computing problems such as Mach reflection problem discussed in the previous section. As is discussed in Woodward [24], the number of timesteps required after the time of reflection for the Mach stem to form increases as does the width of the shock; consequently, the MUSCL code having shocks which are 1-2 zones wide, obtains on coarser meshes comparable results to those obtained here.

There are several directions in which further work is indicated. For one-dimensional flows, Glimm's method with van der Corput sampling is quite effective in modelling the interaction of discontinuities with smooth parts of the flow, without introducing unacceptable errors in the latter. The fact that the solutions to the Riemann problem we use in the numerical scheme satisfy exactly the conservation laws is probably not essential to the accuracy of the method, since much of that information is lost in the sampling. What is essential is that the solution which is sampled has built into it the physically correct waves and wave speeds to some reasonable order

of accuracy. Thus it is feasible to try to model with Glimm's method the dynamics of other media than an ideal gas in Cartesian coordinates: for example, gas dynamics with source terms or unusual equations of state, or elastic-plastic flow.

The central advantage of the hybrid Glimm-Godunov method is that it has the simplicity and stability of a first-order method, with substantially less numerical diffusion than is usually seen in first-order methods. As the method is currently engineered, it seems to be more accurate than the non-adaptive first- and second-order methods, but not as accurate as some of the adaptive methods. The main question to be answered is the determination of a set of optimum engineering decisions. One problem is that we have seen that the criterion for whether to use Glimm's method or Godunov's method at a point is different depending on the strength of the waves; the distinction between strong and weak waves should be made locally, by the algorithm. More generally, although the general principle for switching between the two methods is clear, the actual details of the procedure are still determined in a fairly ad-hoc, problem-dependent fashion, and a more systematic algorithm is needed.

Acknowledgments

Appendix: Calculation of Approximate Solutions to the Riemann Problem

In this appendix, we present a detailed description of the procedure used to calculate approximate values to the solution to the Riemann Problem in the two dimensional hybrid Glimm-Godunov calculations described in Sec. 2. The approximations introduced here are designed to give sufficiently accurate answers for the minimum computational effort in the two situations which arise in those calculations: 1) the sonic waves are weak, or 2) the sonic waves are strong, but the values calculated are used only for computing fluxes in Godunov's method. The algorithm given here is also better suited for efficient implementation on a vector processor, such as the Cray-I, than those given previously.

The first step is an iteration to calculate $p*$, the pressure of the gas between the two sonic waves. We use the Newton's method algorithm given in van Leer [23], with one important modification: we assume that the formulae for $W_{L,R}$, the mean Lagrangian wave speeds, are the same for both shocks and rarefactions:

$$W_{L,R}(p*) = C_{L,R} \sqrt{1 + \frac{\gamma + 1}{2\gamma} \frac{(p* - p_{L,R})}{p_{L,R}}}$$

$$C_{L,R} = \sqrt{\gamma p_{L,R} \rho_{L,R}} = \rho_{L,R} c_{L,R}$$

then the iteration proceeds as follows:

$$p^{*,0} = (C_L p_R + C_R p_L - C_L(u_R - u_L))/(C_L + C_R)$$

$$W_{L,R}^{\ell} = W_{L,R}(p^{*,\ell-1})$$

$$Z_{L,R} = 2(W_{L,R}^{\ell})^3/\left(C_{L,R}^2 + (W_{L,R}^{\ell})^2\right)$$

$$u_L^{*,} = u_L^{\ell} - (p^{*,\ell-1} - p_L)/W_L \; u_L^{*,} \;,\; u_R^{*,\ell} = u_R + (p^{*,\ell-1} - p_R)/W_R$$

$$p^{*,\ell} = p^{*,\ell-1} - Z_L Z_R(u_R^{*,\ell} - u_L^{*,\ell})/(Z_L + Z_R)$$

One criterion for terminating the iteration is to terminate if

$$|p^{*,\ell} - p^{*,\ell-1}|/p^{*,\ell} < \epsilon \qquad .$$

where $\epsilon > 0$ is some predetermined tolerance, and set $p^* = p^{*,\ell}$. In programming this procedure for the Cray-I, we iterated a fixed number of times ℓ_0, i.e. set $p^* = p^{*,\ell_0}$, independent of the left and right states. We obtained more than adequate accuracy using $\ell_0 = 4$, for even the strongest problems; it appears to be sufficient, for a wide class of problems, to set ℓ_0 to be 1 or 2.

Having obtained p*, we calculate the other quantities we will need

$$W_{L,R} = W_{L,R}(p*)$$

$$u* = (p_L - p_R + u_L W_L + u_R W_R)/(W_L + W_R)$$

If, at any point in the iteration, $p^{*,\ell} < 0$, we reset to be equal to some floor value $1 \gg p_{min} > 0$. If $p^{*,\ell} < 0$ for two iterations in a row, we terminate the iteration (or ignore the results) setting $p* = p_{min}$.

The second part of the procedure is to calculate the value of the solution at some given point (x,t); we denote the values of the pressure density, velocity, and passive component of the velocity at that point by p, ρ, u, v. We follow the procedure given in [3], but use explicitly the reflection symmetry of the equations to consolidate some of the formulae.

Let $\psi = \frac{x}{t}$ and $s = sgn(\psi - u*)$. The we define

$$(u_0, p_0, \rho_0, W_0, c_0, v) = (u_L, p_L, \rho_L, W_L, c_L, v_L) \quad \text{if} \quad s = -1$$

$$= (u_R, p_R, \rho_R, W_R, c_R, v_R) \quad \text{if} \quad s = 1$$

$$\bar{u}_0 = su_0 \quad \bar{\psi} = s\psi, \quad \bar{u}* = su*$$

We then compute

$$\rho* = (\rho_0^{-1} - (p* - p_0)/W_0^2)^{-1} \quad , \quad c* = \sqrt{\frac{\gamma p*}{p*}}$$

$$\lambda_0, \lambda* = u_0 + c_0, \ u* + c* \qquad \text{if} \qquad p* < p_0$$

$$= \bar{u} + \frac{W_0}{\rho_0} \qquad \text{if} \qquad p* > p_0$$

We evaluate p, ρ, u as follows:

$$p, \rho, u = p*, \rho*, u* \qquad \text{if} \qquad \bar{\psi} \geq \lambda*$$

$$= p_0, \rho_0, u_0 \qquad \text{if} \qquad \bar{\psi} < \lambda_0$$

if $\lambda_0 < \bar{\psi} < \lambda$, then the solution is being evaluated inside a centered rarefraction wave, and we have

$$c = \bar{\psi} - \bar{u}* + \frac{2c*}{\gamma - 1} \ \frac{\gamma - 1}{\gamma + 1}$$

$$u = s(\bar{\psi} - c)$$

$$\rho = \left(\frac{c}{c_0}\right)^{\frac{2}{\gamma - 1}} \rho_0$$

$$p = \frac{\rho c^2}{\gamma}$$

One can replace the expression for ρ inside a rarefaction fan by the formula

$$\rho = \rho_0 \; \frac{1 - \alpha}{1 + \alpha} \; , \quad \alpha = \frac{1}{\gamma - 1} \; \frac{c_0^2 - c^2}{c_0^2 + c^2}$$

which does not require evaluation of a rational power.

If the iteration is carried out to convergence, all the approximations introduced here are correct to third order in the pressure jump across the strongest rarefaction wave present. If one of the waves is a strong rarefaction, we will be using the results to calculate fluxes for Godunov's method, and the error committed by using the rarefaction shock formula in the iteration is lost in the averaging. However, it is essential to evaluate the solution inside the rarefaction fans, rather than treating the waves as jump discontinuities, as is done in [13]. Otherwise, sampling would not spread weak rarefactions; nor would the averaging in Godunov's method spread strong rarefaction shocks into rarefaction waves, if the speed of the rarefaction shock is close to zero.

Using similar approximations to those used above in computing the solution to the Riemann problem, we extend the sampling procedure to the case where the timestep satisfies (3.1) for $\frac{1}{2} < \sigma < 1$, assuming that the sonic waves in the solution being sampled are weak. The procedure described below accounts correctly for the possible interpenetration of waves from successive Riemann problems to first order in the strengths of the sonic waves, and reduces to the previous sampling procedure when the waves do not intersect.

To update the solution at zone j, we first evaluate at $((j - \frac{1}{2} + a^{n+1}) \Delta x,$ $(n+1)\Delta t)$ the solution to the Riemann problems on either side of the zone:

$$U_{+,j}^{n+1} = h_{j-\frac{1}{2},n}\left(a^{n+1}\,\frac{\Delta x}{\Delta t}\right)$$

$$U_{-,j}^{n+1} = h_{j+\frac{1}{2},n}\left((a^{n+1}\,-\,1)\,\frac{\Delta x}{\Delta t}\right)$$

$U_{+,j}^{n+1} = U_{j-1}^{n}$ or U_{j}^{n} or $U_{-,j}^{n+1} = U_{j}^{n}$ or U_{j+1}^{n} then we can assume, since

the sonic waves are weak, that the waves from the Riemann probles at

$((j-\frac{1}{2})\Delta x, n\Delta t)$ and $((j+\frac{1}{2})\Delta x, n\Delta t)$ do not intersect, and set

$$\left(U_j^{n+1}\right)_{\text{Glimm}} \quad \begin{array}{ll} = U_{-,j}^{n+1} & \text{if} \quad U_{+,j}^{n+1} = U_j^n \\[1em] = U_{+,j}^{n+1} & \text{otherwise} \end{array}$$

If $U_{+,j}^{n+1} \neq U_j^n$, U_{j-1}^n and $U_{-,j}^{n+1} \neq U_j^n, U_{j+1}^n$, then we assume that the

waves contained in the jump $(U_{+,j}^{n+1}, U_j^n)$ have reached and interacted

with the waves contained in the jump $(U_j^n, U_{-,j}^{n+1})$. Using again the

assumption that the sonic waves are weak, we see that the waves which

intersect are: a part of a backwards-facing sonic wave, from the Riemann

problem at $((j+\frac{1}{2})\Delta x, n\Delta t)$; a part of the forwards facing sonic wave from the

Riemann problem at $((j-\frac{1}{2})\Delta x, n\Delta t)$ and at most one contact discontinuity, which

might come from either one of the Riemann problems (figure A1). In that case,

we calculate $(p_j^{n+1},\ \rho_j^{n+1},\ u_j^{n+1},\ v_j^{n+1})_{\text{Glimm}}$ as follows:

$$W_R = W_{R,j-\frac{1}{2}}^{n+1}\ \sqrt{\gamma p_{-,j}^{n+1}\ \rho_{-,j}^{n+1}}\ \Big/\ \sqrt{\gamma p_j^n \rho_j^n}$$

$$W_L = W_{L,j+\frac{1}{2}}^{n+1} \sqrt{\gamma p_{+,j}^{n+1} \rho_{+,j}^{n+1}} \Big/ \sqrt{\gamma p_j^n \rho_j^n}$$

$$p_j^{n+1} = \left(W_R p_{-,j}^{n+1} + W_L p_{+,j}^{n+1} - W_L \times (u_{+,j}^{n+1} - u_{-,j}^{n+1})\right) \Big/ (W_L + W_R)$$

$$u_j^{n+1} = u_{+,j}^{n+1} + W_R (p_j^{n+1} - p_{+,j}^{n+1})$$

$$\rho_j^{n+1} = \left((\rho_{+,j}^{n+1})^{-1} - (p_j^{n+1} - p_{+,j}^{n+1}) \; W_R^2\right)^{-1}$$

$$v_j^{n+1} = v_{+,j}^{n+1}$$

$$\text{if} \quad (a^{n+1} - 1)\frac{\Delta x}{\Delta t} < u_{j+\frac{1}{2}}^{*,n+1}$$

$$\rho_j^{n+1} = \left((\rho_{-,j}^{n+1})^{-1} - (p_j^{n+1} - p_{-,j}^{n+1}/W_L^2)\right)^{-1}$$

$$v_j^{n+1} = v_{-,j}^{n+1}$$

$$\text{otherwise}$$

Here $W_{L,j+\frac{1}{2}}^{n+1}$, $W_{R,j-\frac{1}{2}}^{n+1}$, $u_{j+\frac{1}{2}}^{*,n+1}$ are the mean Lagrangian wave
speeds and the velocity of the gas between the two sonic waves for Riemann
problems centered at $((j+\frac{1}{2})\Delta x, n\Delta t)$.

The above scheme can be implemented in such a way that almost all the
calculations are vectorizable. For the test problems discussed in Sec. 4, a
program run on the Cray-I at the LLNLCC, compiled using the CFT compiler, took
about 14 μs/zone/time step/space dimension, or about 35,000 zones/second for a
two dimensional problem. The iteration scheme for computing p*,u* is done

once per zone, independent of whether one is sampling or averaging in that zone, and takes $(1.7 + 1.15 \times \ell_0)$ µs = 4 µs for ℓ_0 = 2, or less than one-third of the time per timestep. A good deal of redundant work is performed because of the limited number of vectorized logical operations available at the Fourtran level using the CFT compiler. As more of the Cray-I's capabilities become accessible, such as vectorized gather/scatter operations and bit vector logic, the timings should improve substantially.

References

[1]   N. Albright, P. Concus, and W. Proskurowski, "Numerical Solution of the Multidimensional Buckley-Leverett Equation by a Sampling Method," Report No. LBL-8452, Lawrence Berkeley Laboratory, University of California (1978).

[2]   J. P. Boris and D. L. Book, "Flux-Corrected Transport. I. SHASTA, A Fluid Transport Algorithm That Works," J. Computational Phys. $\underline{23}$ (1973), p. 38-69.

[3]   A. J. Chorin, "Random Choice Solution of Hyperbolic Systems," J. Computational Phys. $\underline{22}$ (1976), p. 517-536.

[4]   A. J. Chorin, "Random Choice Methods with Application to Reacting Gas Flow," J. Computational Phys. $\underline{25}$ (1977) p. 252-272.

[5]   P. Colella, "An Analysis of the Effect of Operator Splitting and of the Sampling Procedure on the Accuracy of Glimm's Method," Ph. D. Dissertation, University of California, Berkeley, June 1979.

[6]   P. Colella, "Error Analysis of Glimm's Method," to appear.

[7]   P. Concus and W. Proskurowski, "Numerical Solution of a Nonlinear Hyperbolic Equation by a Random Choice Method," J. Computational Phys. $\underline{30}$ (1979), p. 153-166.

[8]   R. Courant and K. O. Friedrichs, Supersonic Flow and Shock Waves, Interscience, New York, 1948.

[9]   J. Glimm, "Solution in the Large for Nonlinear Hyperlinear Systems of Equations," Comm. Pure Appl. Math. $\underline{18}$ (1955), p. 697-715.

[10]   J. Glimm, D. Marchesin, O. McBryan, "A Numerical Method for Two Phase Flow with an Unstable Interface," preprint.

[11]   J. Glimm, D. Marchesin, E. Isaacson, and O. McBryan, "A Shock Track-
        ing Method for Hyperbolic Systems," preprint.

[12]   S. K. Godunov, "Difference Methods for the Numerical Calculations of
        Discontinuous Solutions of the Equations of Fluid Dynamics," Math.
        Sb. 47 (1959) p. 271-306 (in Russian).

[13]   S. K. Godunov, A. V. Zabrodin, and G. P. Prokopov, "A Computational
        Scheme for Two-Dimensional Non Stationary Problems of Gas Dynamics
        and Calculations of the Flow from a Shock Wave Approaching a Station-
        ary State," USSR Computational Math. and Math. Phys. 1, (1961), p.
        1187-1218.

[14]   J. M. Hammersley and D. C. Handscomb, Monte Carlo Methods, Methuen,
        London, 1965.

[15]   A. Harten, "The Method of Artificial Compression: I. Shocks and Con-
        tact Discontinuities," AEC Research and Development Report COO-3077-
        50, Courant Institute for the Mathematical Sciences, New York Univer-
        sity (1974).

[16]   A Harten and G. Zwas, "Self-Adjusting Hybrid Schemes for Shock Compu-
        tations," J. Computational Phys. 9, (1972), p. 568-583.

[17]   P. D. Lax, "Hyperbolic Systems of Equations and Computing, SIAM
        Review 11, (1969), p. 7-19.

[18]   F. H. Maltz and D. L. Hitzl, "Variance Reduction in Monte Carlo Com-
        putations using Multidimensional Hermite Polynomials," J. Computa-
        tional Phys. 32 (1979), p. 345-376.

[19]   R. Richtmyer and K. Morton, Difference Methods for Initial-Value
        Problems," 2nd ed., Interscience, New York, 1967.

[20]   G. A. Sod, "A Numerical Study of a Converging Cylindrical Shock," J. Fluid. Mech. 83 (1977), pt. 4, pp. 785-794.

[21]   G. A. Sod, "A Survey of Several Finite Difference Methods for Systems of Nonlinear Hyperbolic Conservation Laws," J. Computational Phys. 27 (1978), pp. 1-31.

[22]   G. A. Sod, "A Numerical Method for a Slightly Vicous Axisymmetric Flow with Application to Internal Combustion Engines," Report No. LBL-9049, Lawrence Berkeley Laboratory, University of California, Berkeley (1979).

[23]   B. van Leer, "Towards the Ultimate Conservative Difference Scheme," V. A. Second Order Sequel to Godunov's Methods, J. Computational Phys. 32 (1979) pp. 101-136.

[24]   P. Woodward, "Comparison of Difference Schemes for Compressible Gas Dynamics and a Framework for New Schemes of High Resolution," in preparation.

[25]   S. T. Zalesak, "Fully Multidimensional Flux-Corrected Transport Algorithms for Fluids," J. Computational Phys. 31 (1979), pp. 335-362.

List of Figures

Figure 1.

Figure 2.

Figure 3.

$$U_j^{n+1} = U_n^e((j-1/2+a^{n+1})\Delta x, (n+1)\Delta t)$$

$((j-1/2+a^{n+1})\Delta x, (n+1)\Delta t)$

$(n+1)\Delta t$

$$U^{(\Delta x)}(x,t) = U_n^e(x,t)$$
$$n\Delta t \leq t \leq (n+1)\Delta t$$

$n\Delta t$

$(j-1/2)\Delta x$ U_j^n $(j+1/2)\Delta x$

Figure 4.

Figure 5.

Figure 6.

Figure 7.
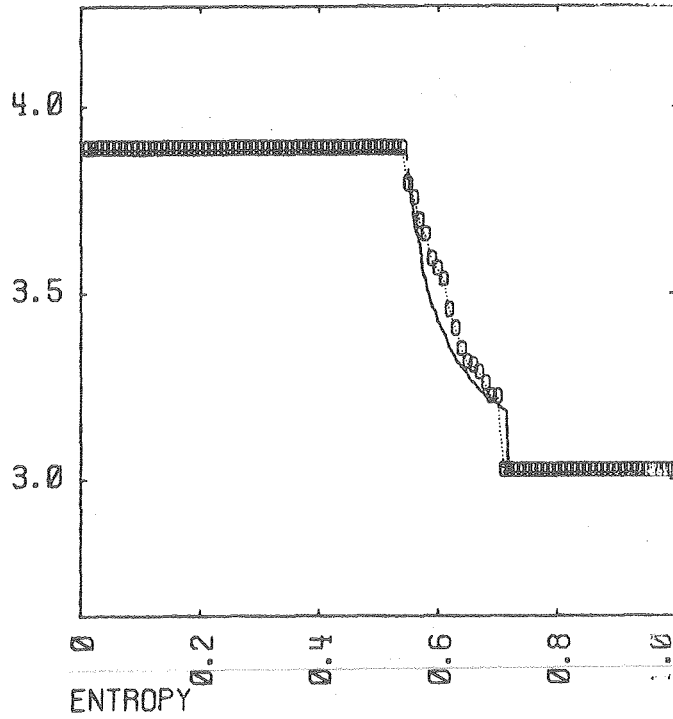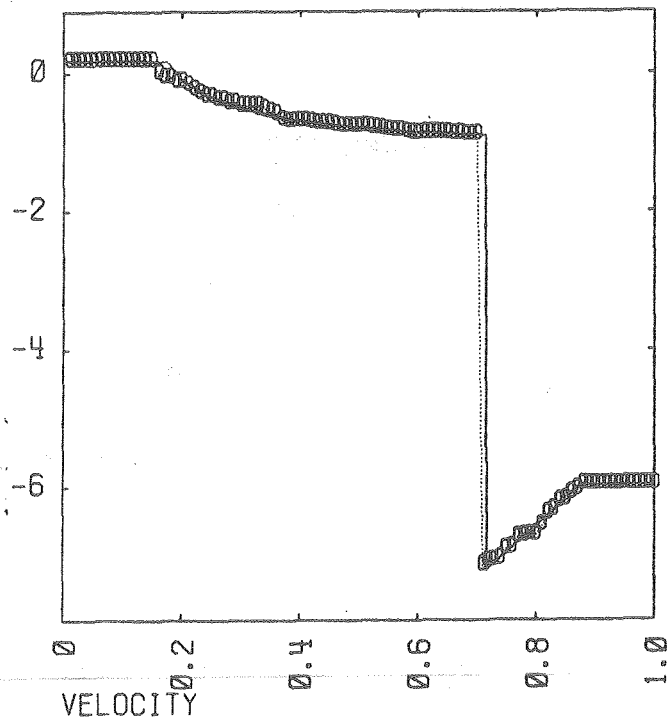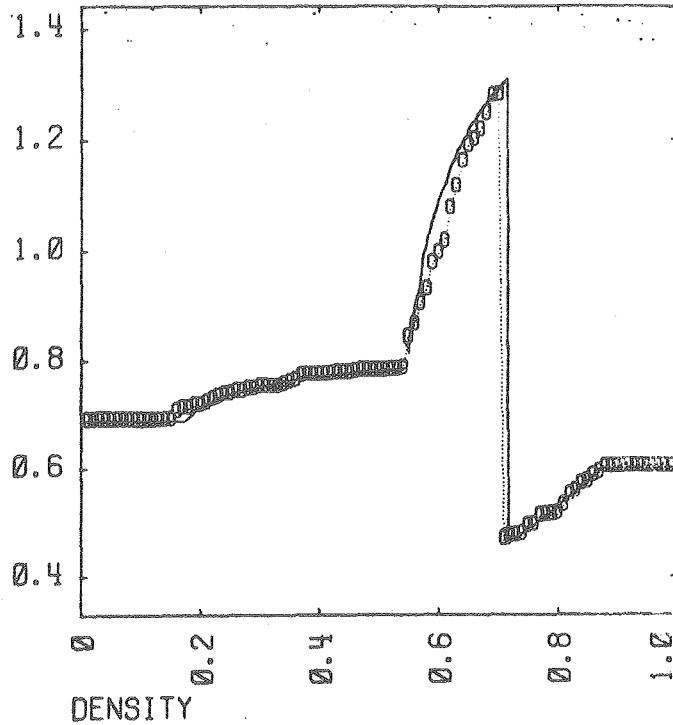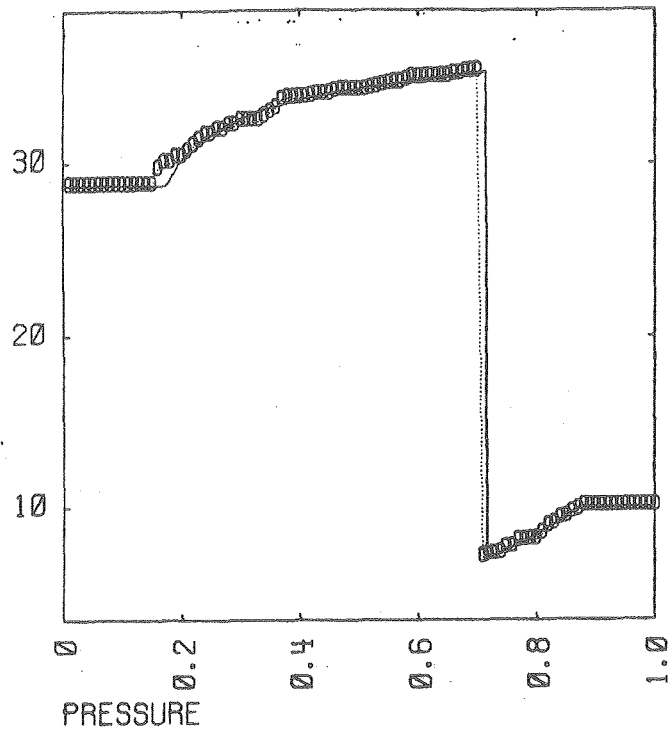
Figure 8.

Figure 9.

Figure 10.

PRESSURE

DENSITY

NORMAL VELOCITY

INTERNAL ENERGY
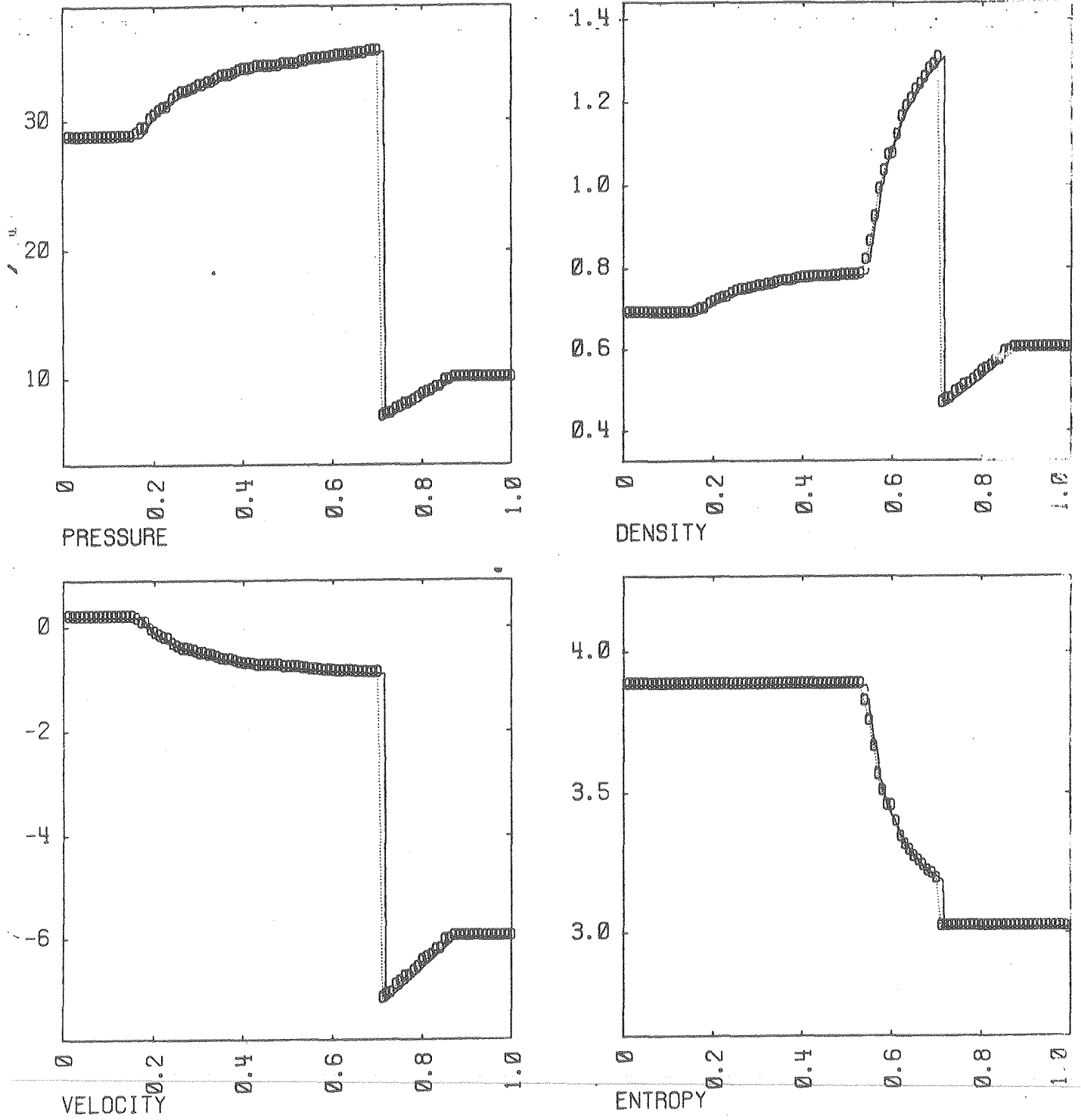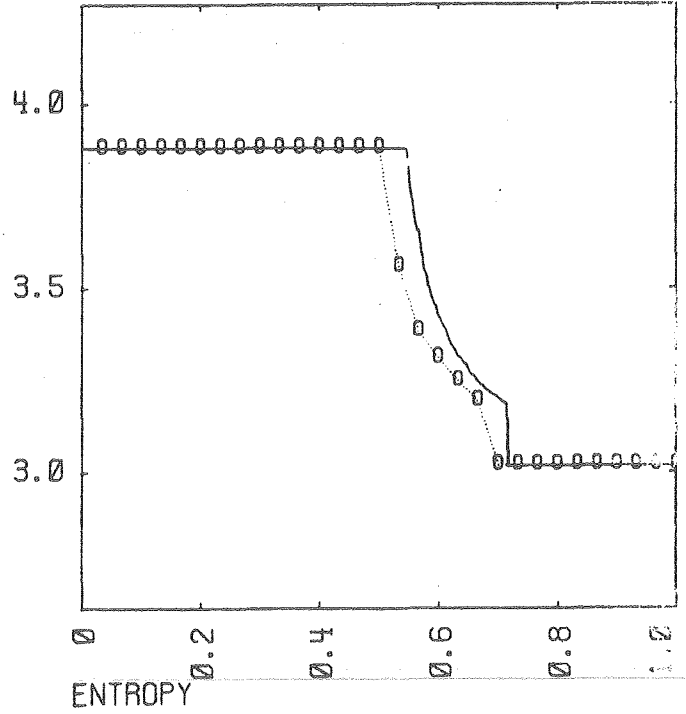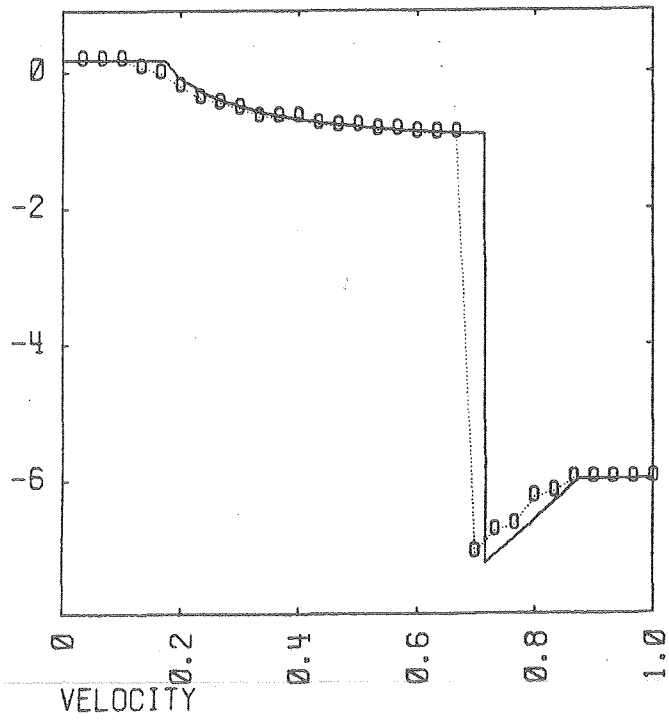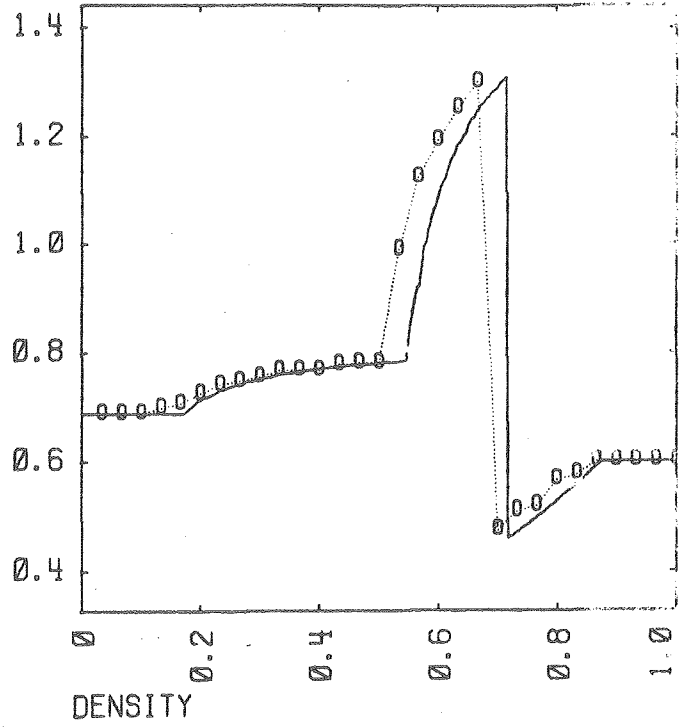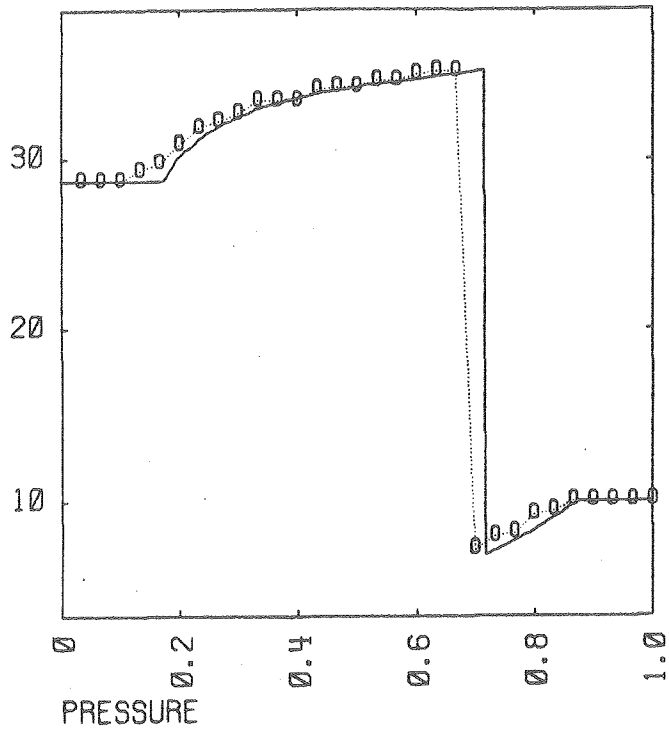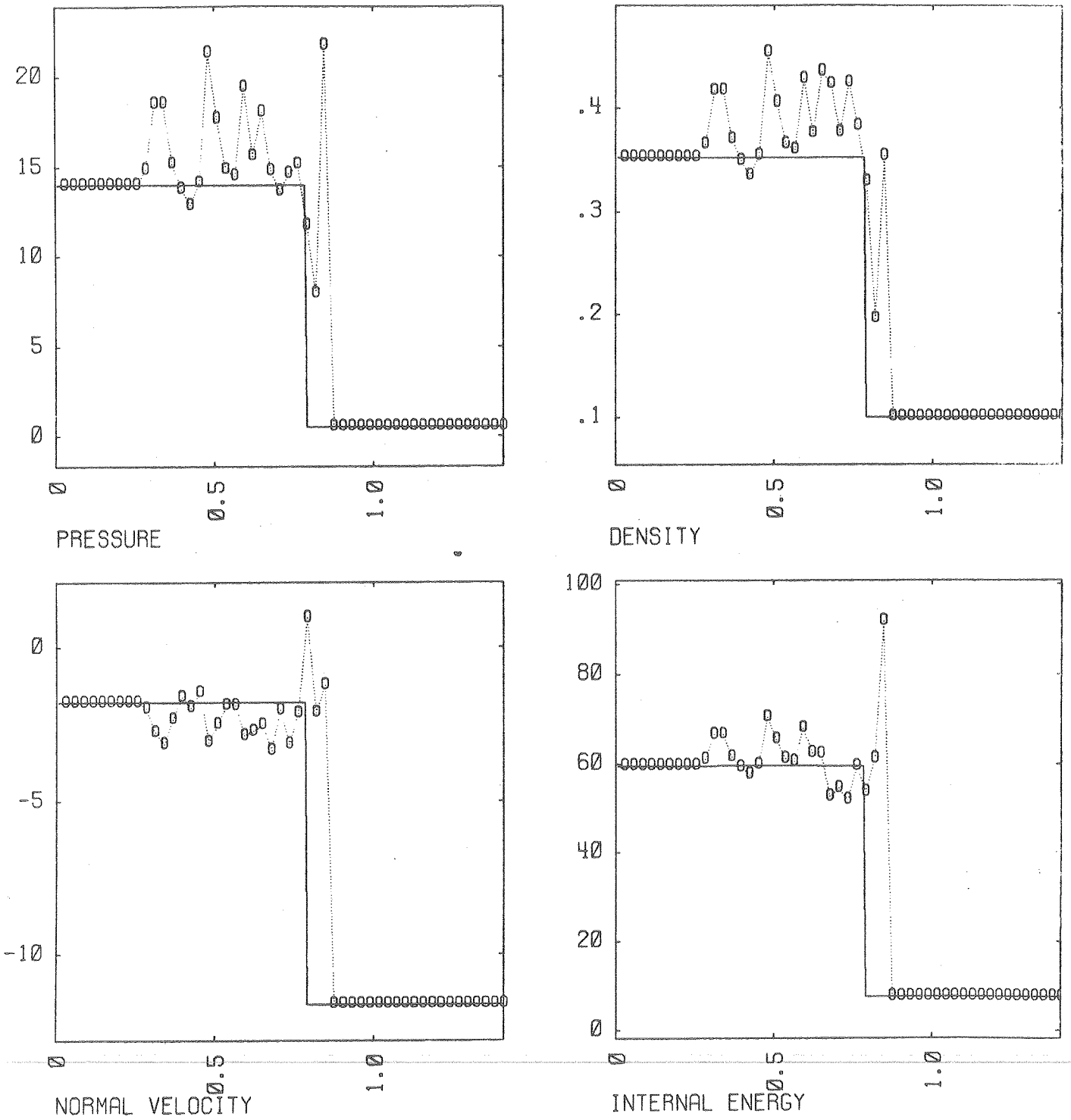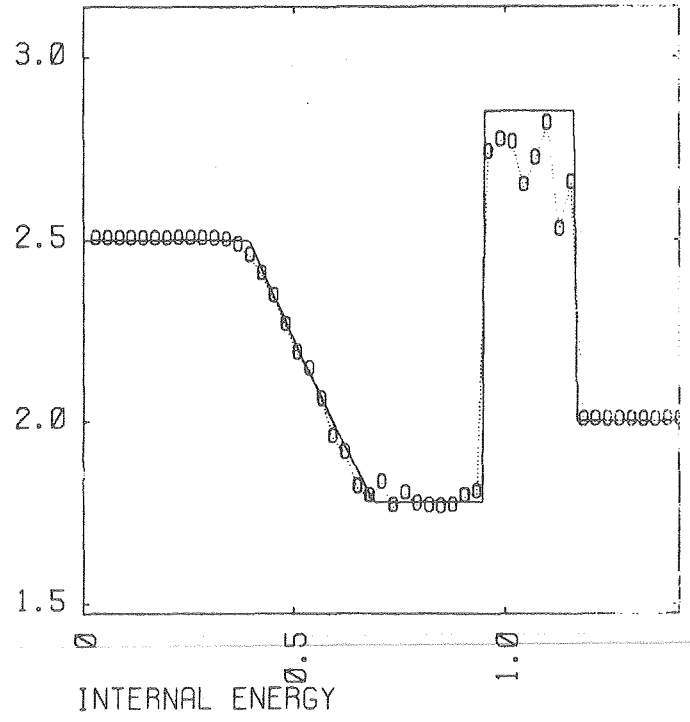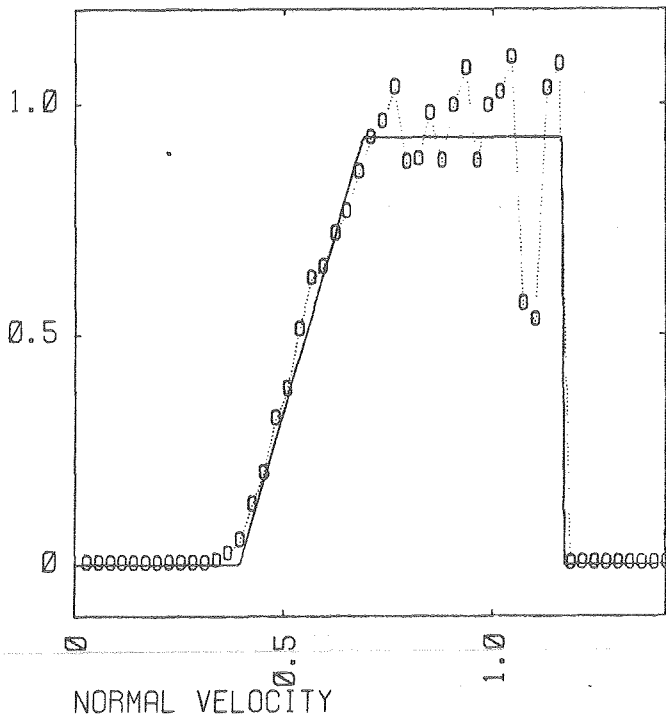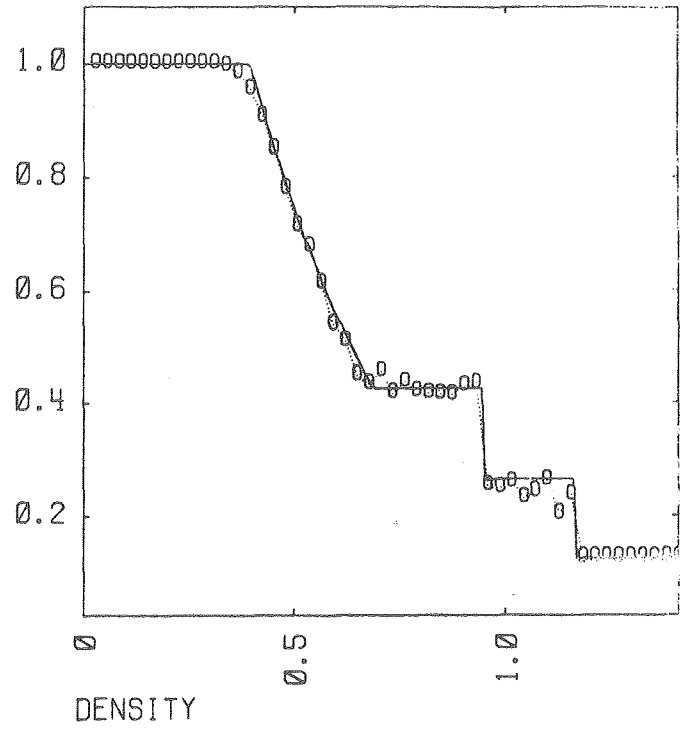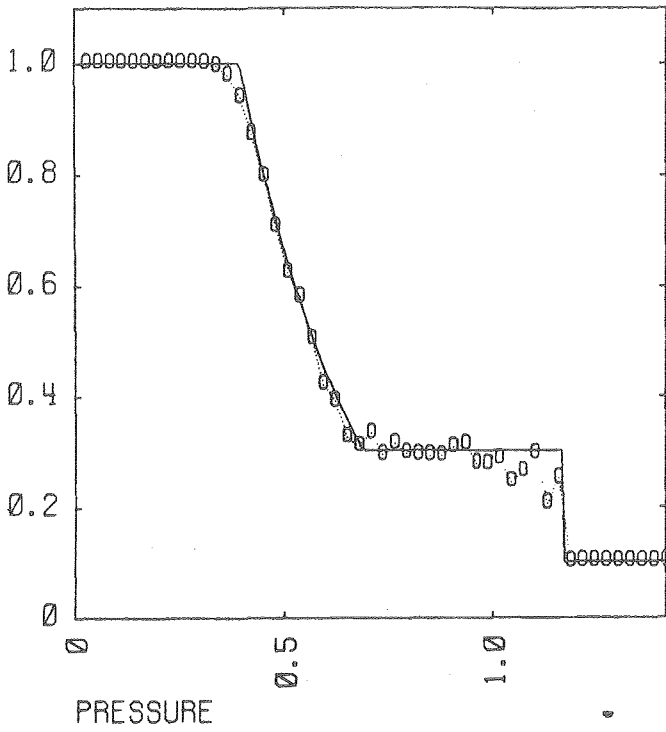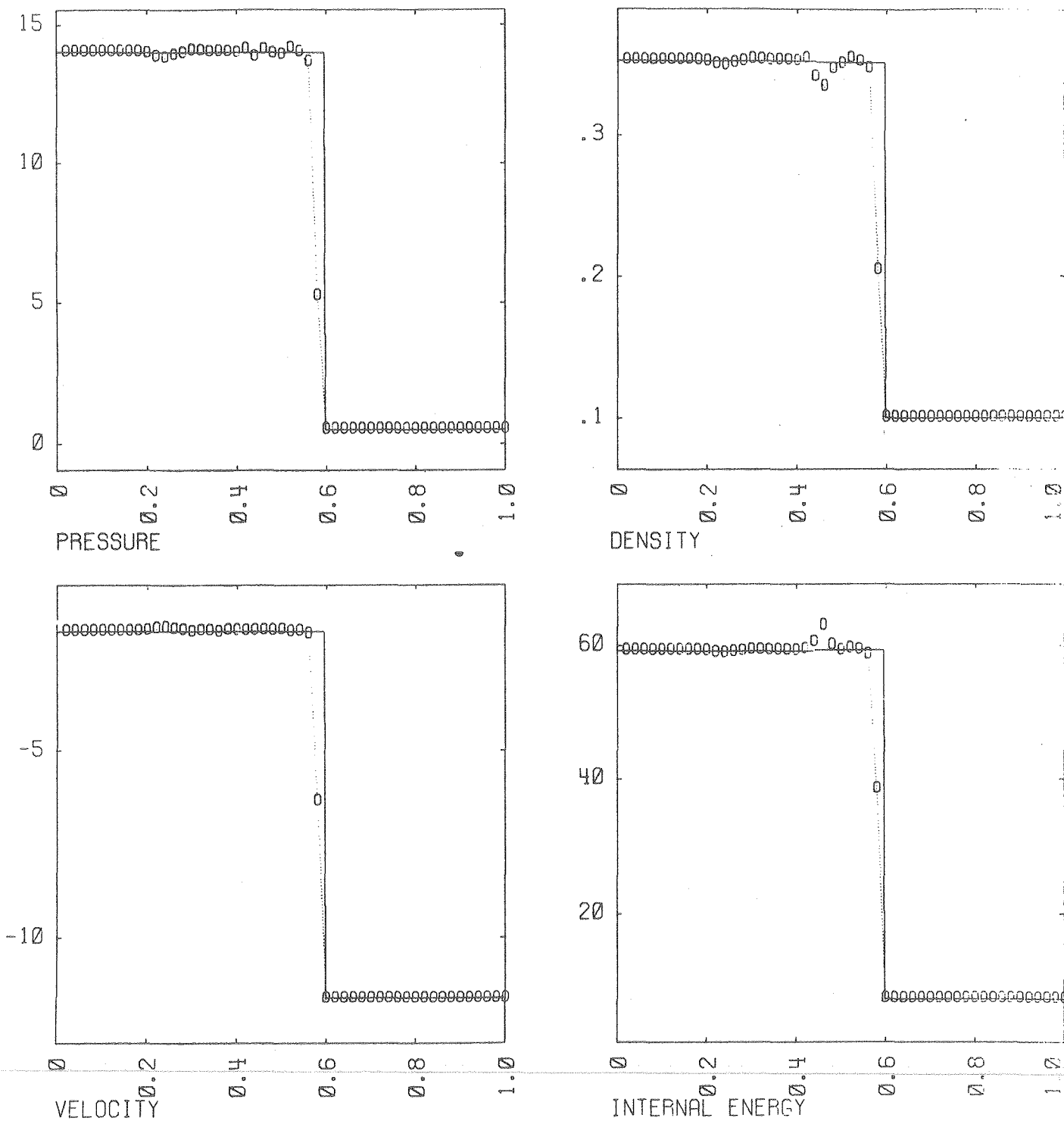
Figure 11.

Figure 12.

Figure 13.
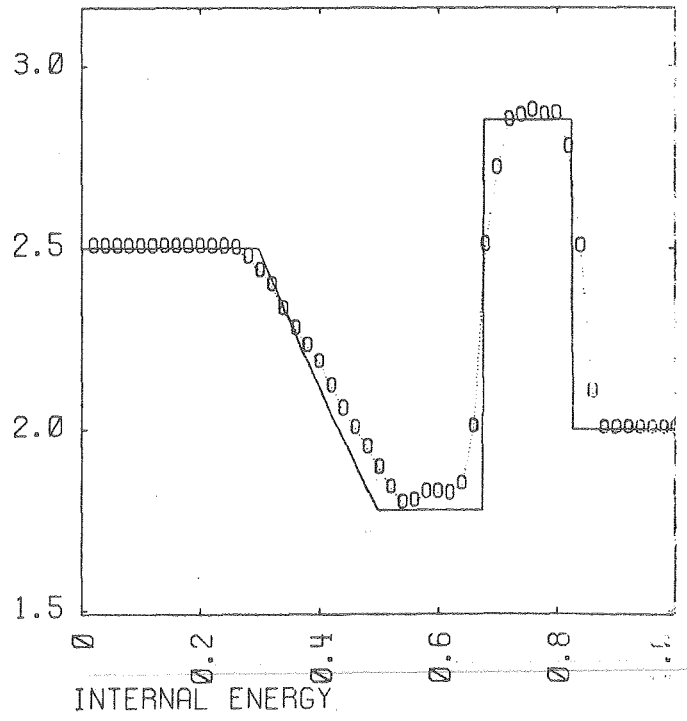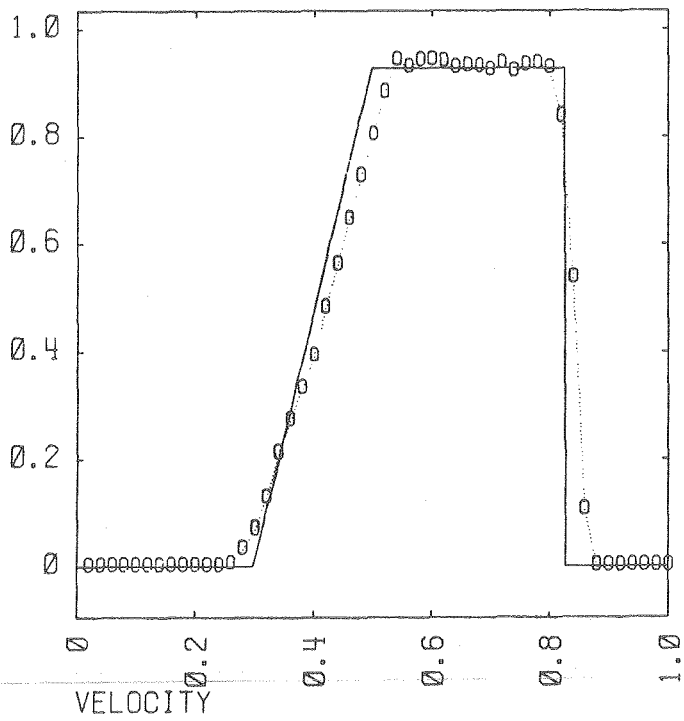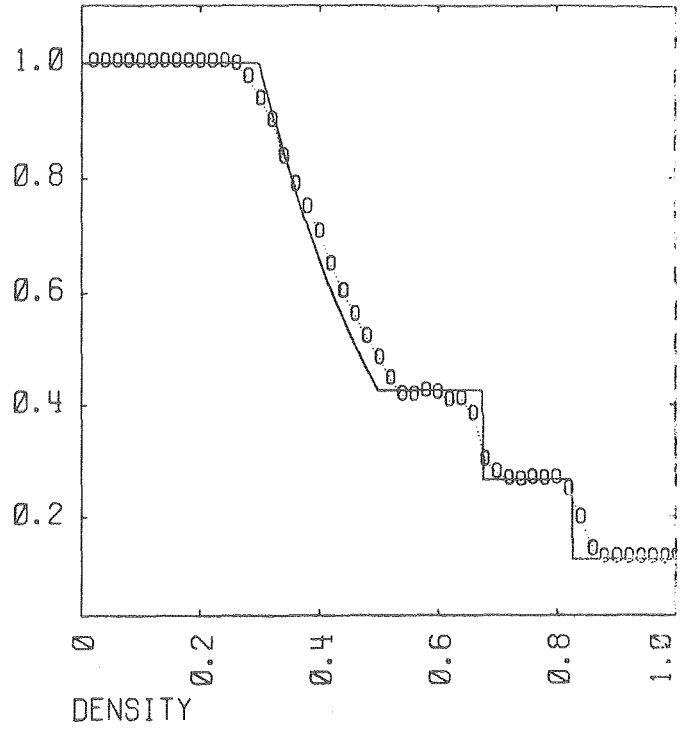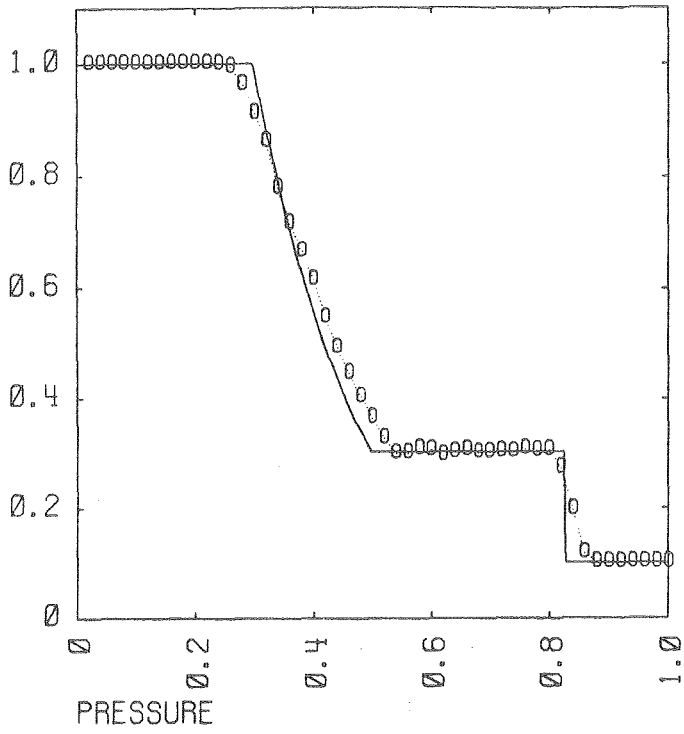
Figure 14.
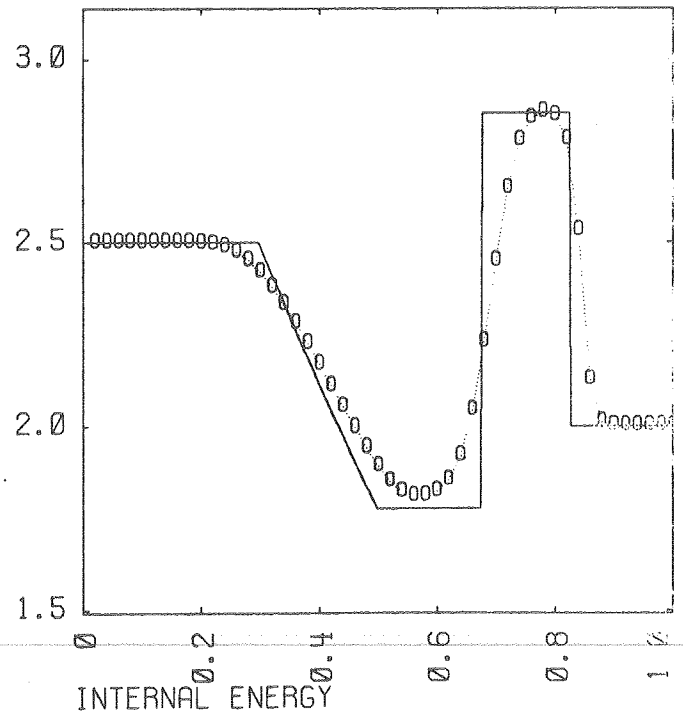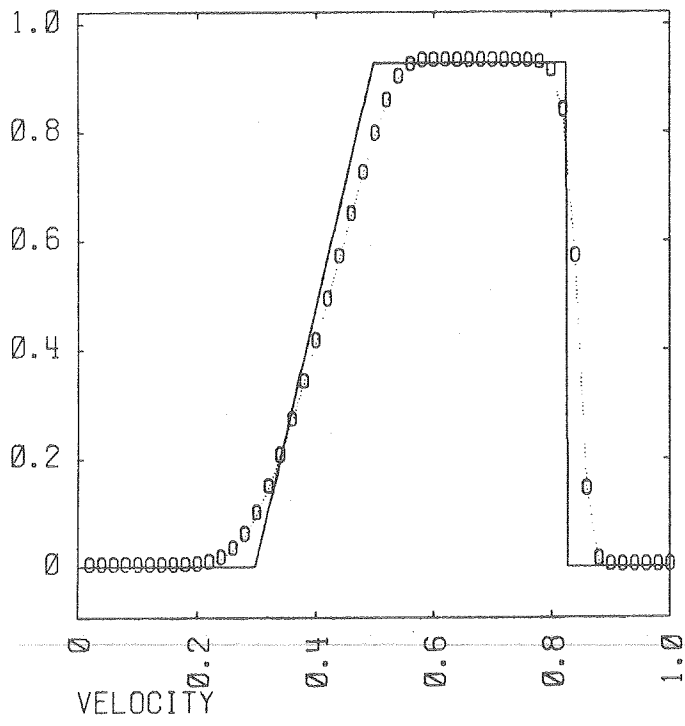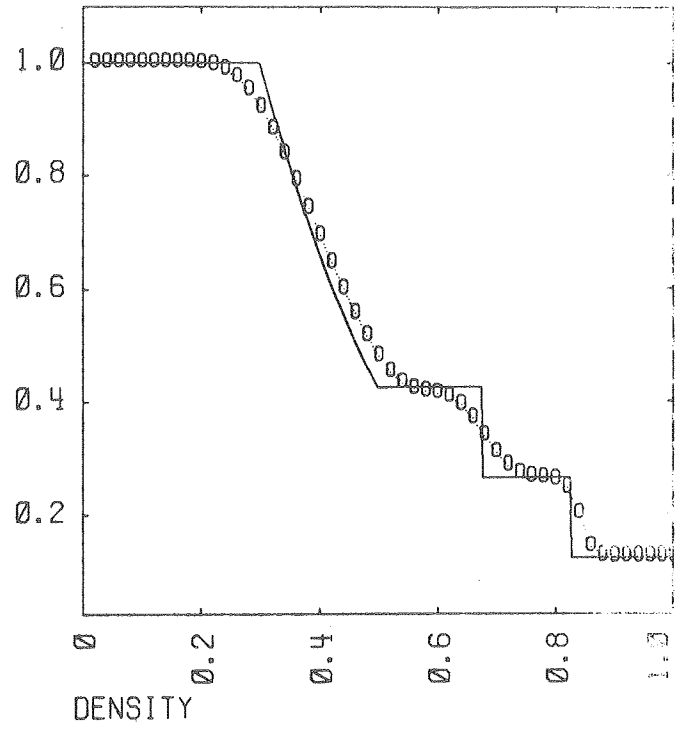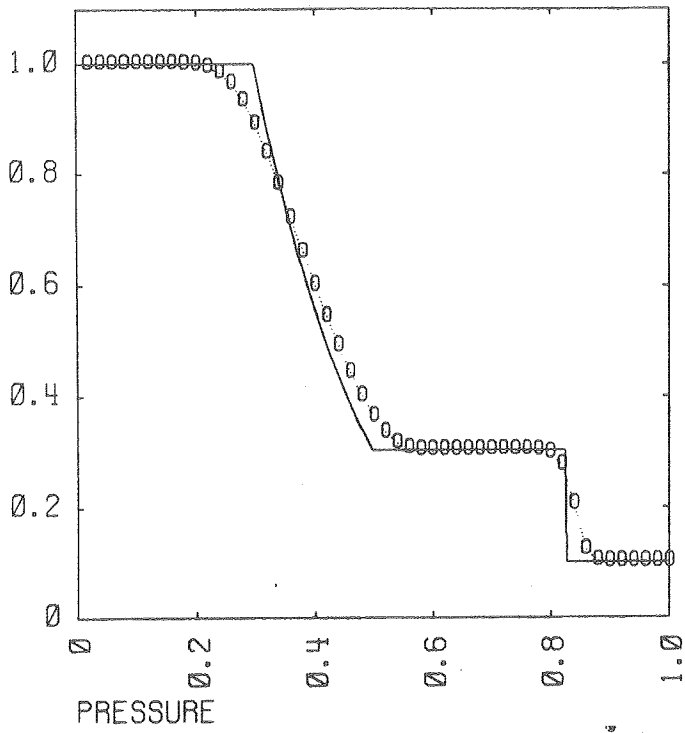
Figure 15.

Figure 16.

DT = 1.389E-03 TIME = 1.334E+00 TIMESTEP = 478 NO. CONTOURS = 30

KIN ENERGY

MIN = 2.80E-02
MAX = 3.00E+00

INT ENERGY

MIN = 1.79E+00
MAX = 5.13E+00

DENSITY

MIN = 6.11E-01
MAX = 6.78E+00

PRESSURE

MIN = 6.62E-01
MAX = 1.21E+01

KIN ENERGY   INT ENERGY   DENSITY   PRESSURE
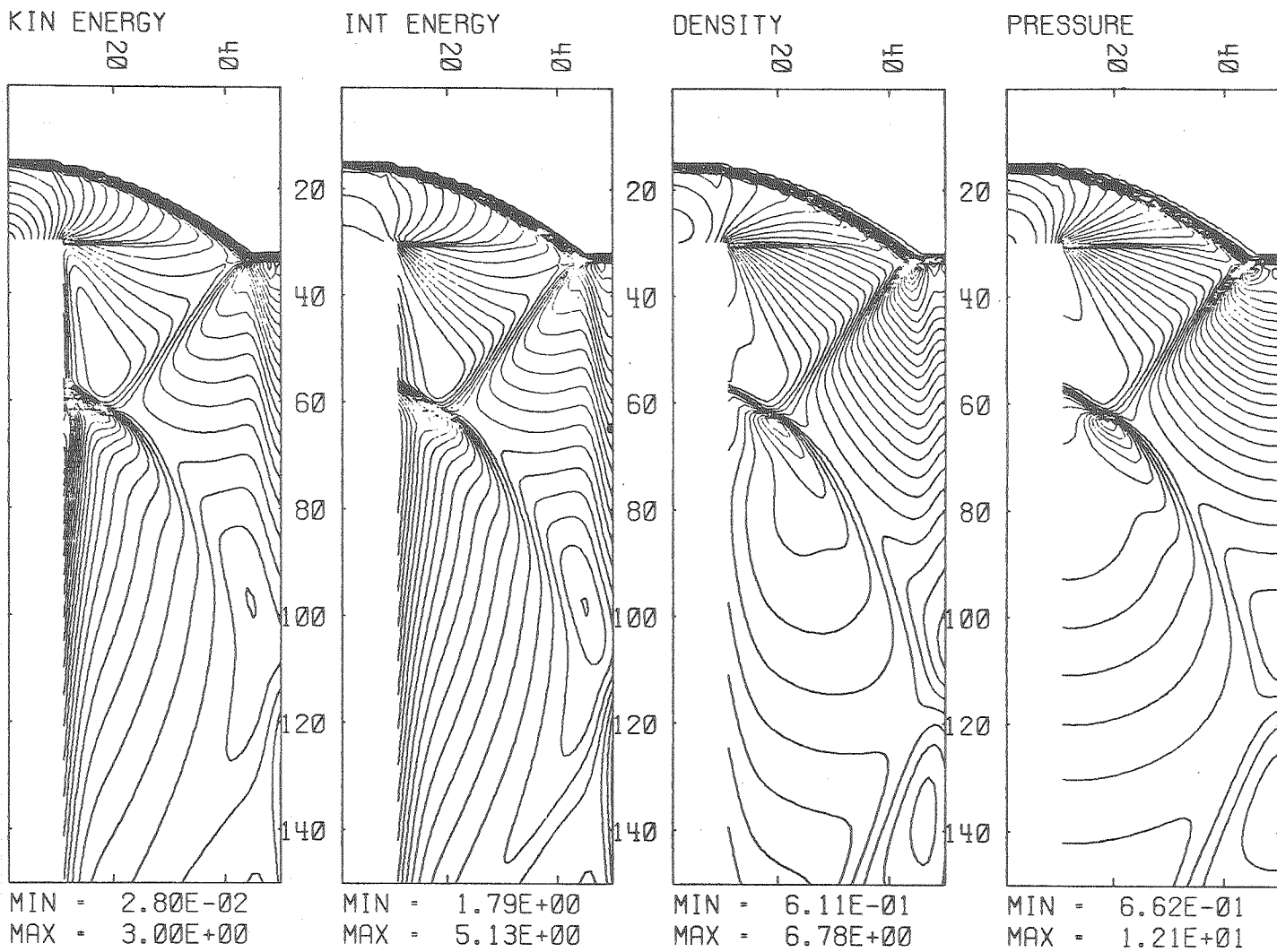
DT = 1.322E-03 TIME = 1.334E+00 TIMESTEP = 496 NO. CONTOURS = 30
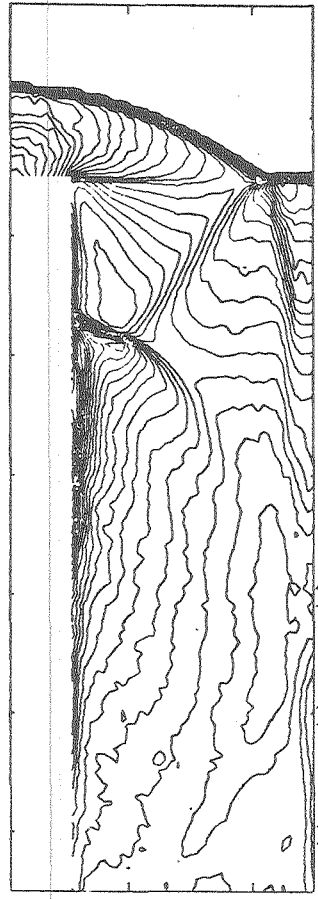
MIN = 0.
MAX = 3.00E+00
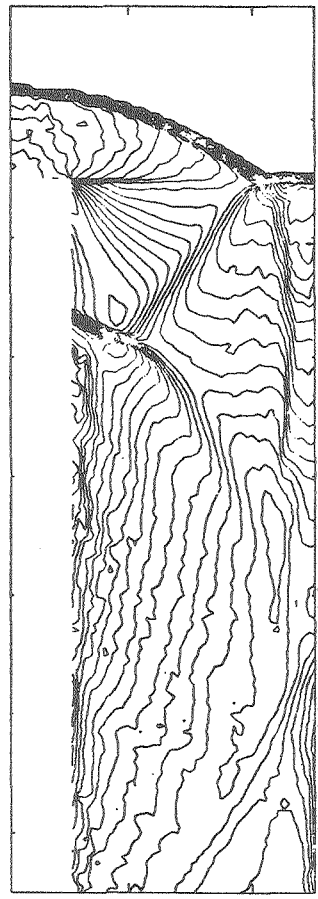
MIN = 1.79E+00
MAX = 5.28E+00
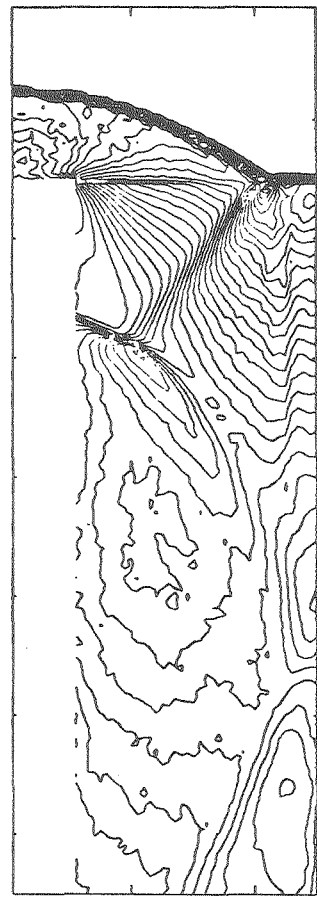
MIN = 5.45E-01
MAX = 6.63E+00
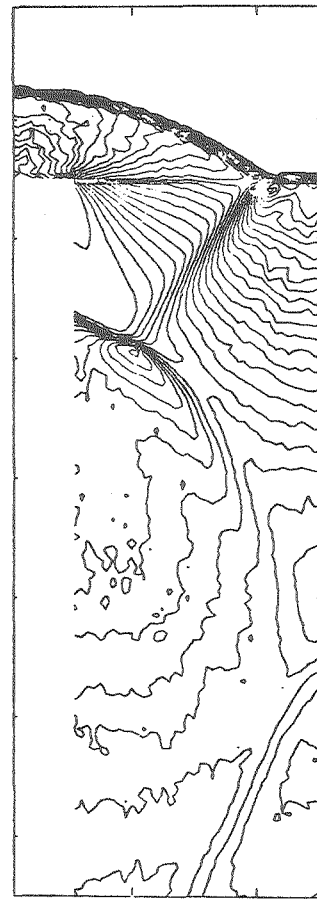
MIN = 5.73E-01
MAX = 1.31E+01
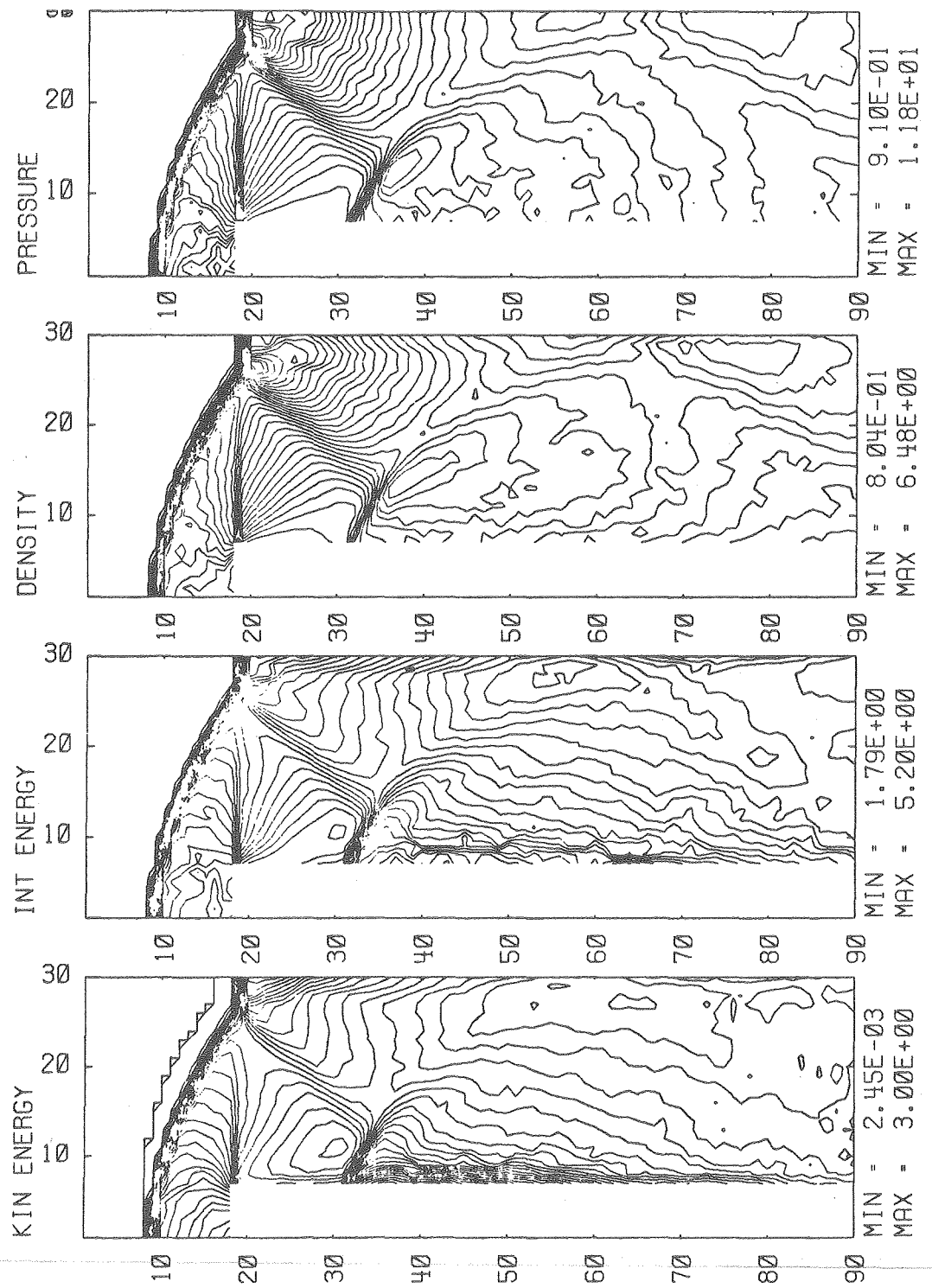
Figure 17.

-70-
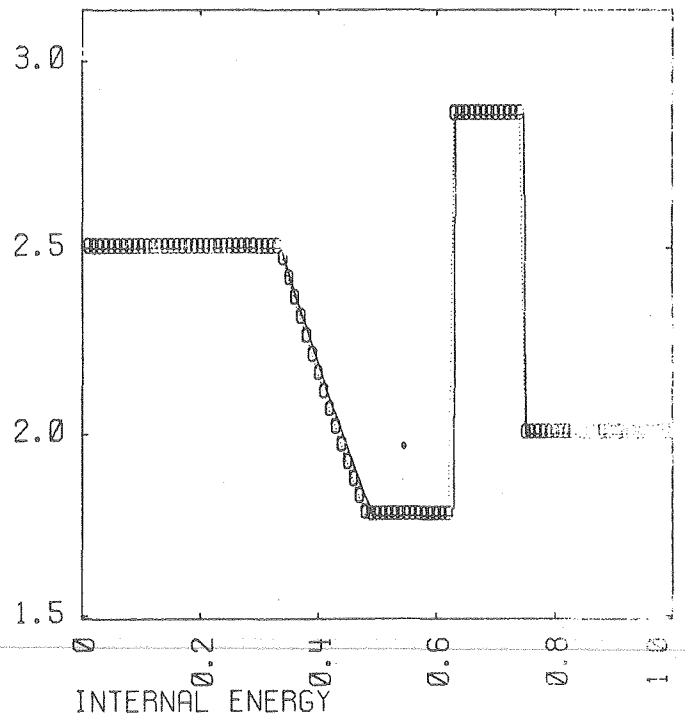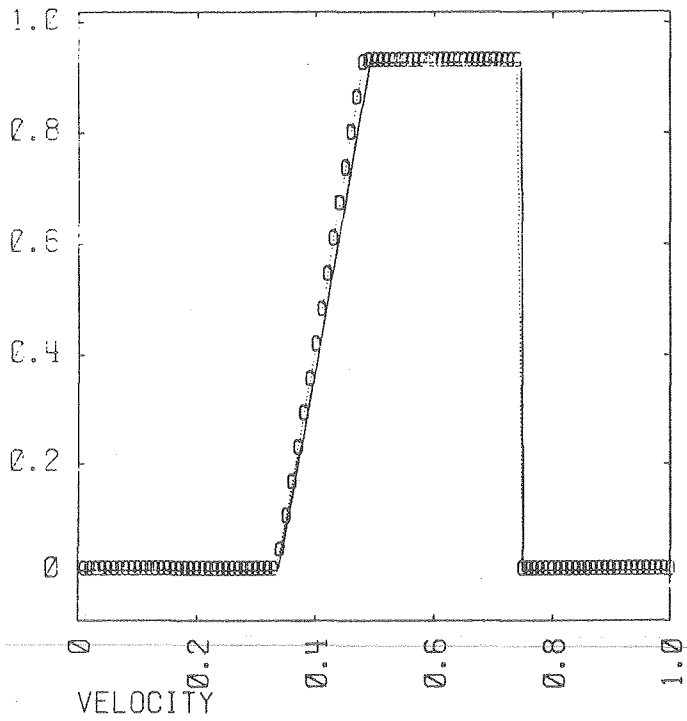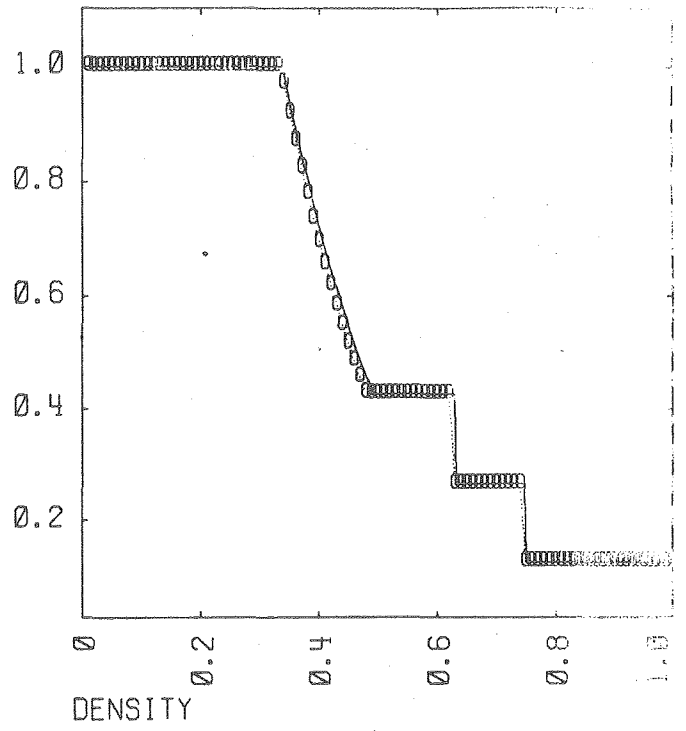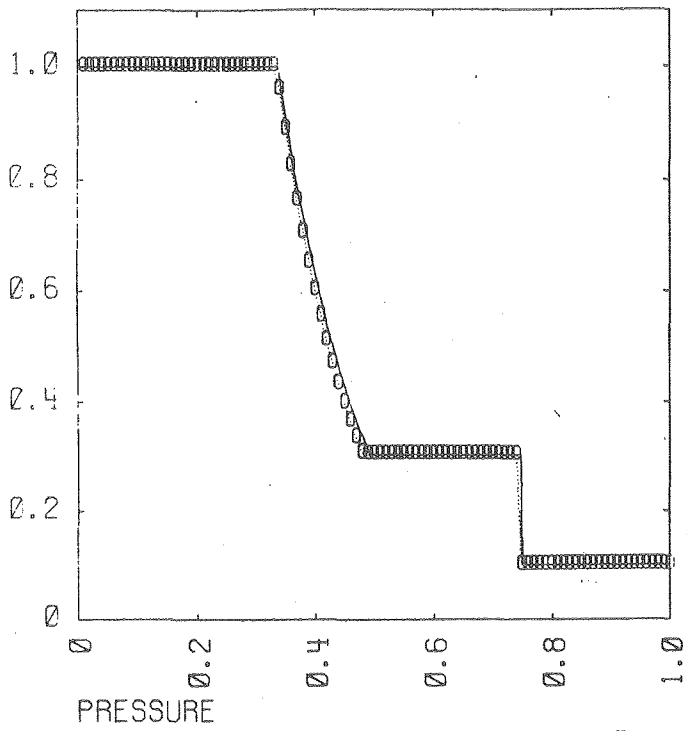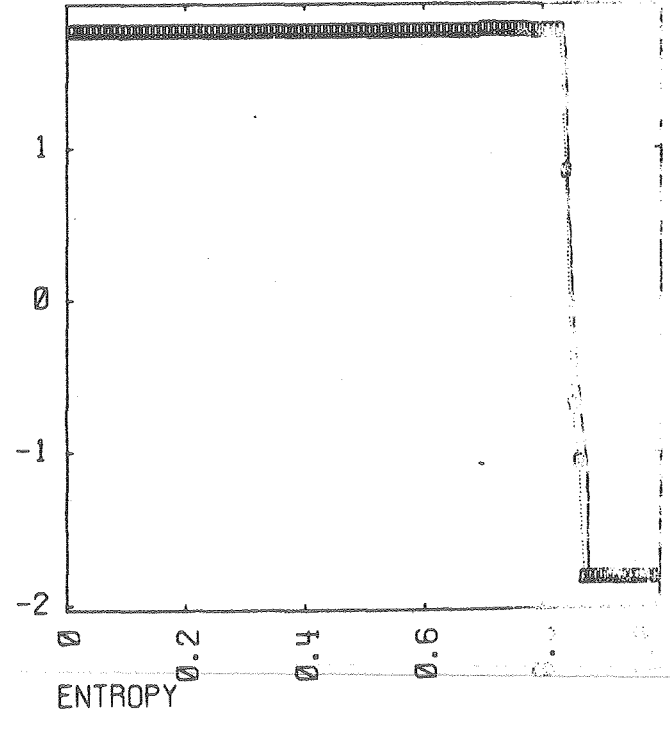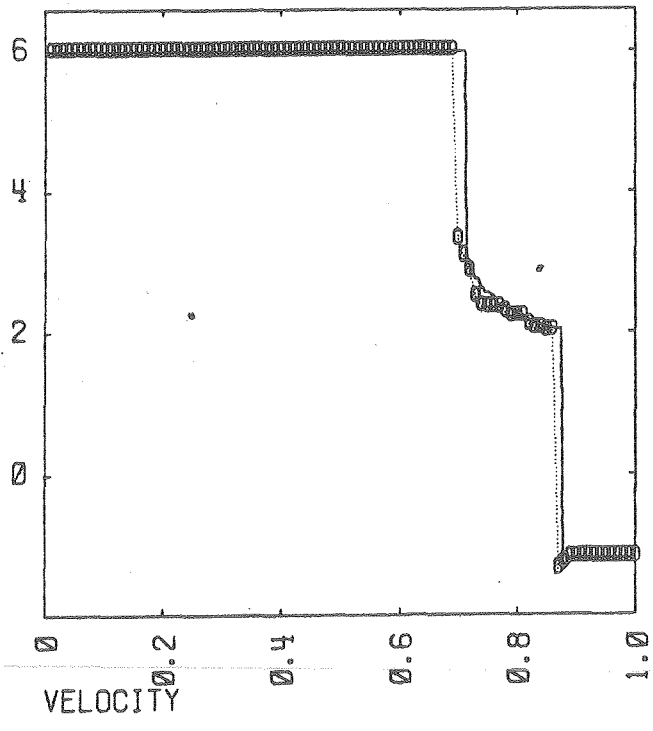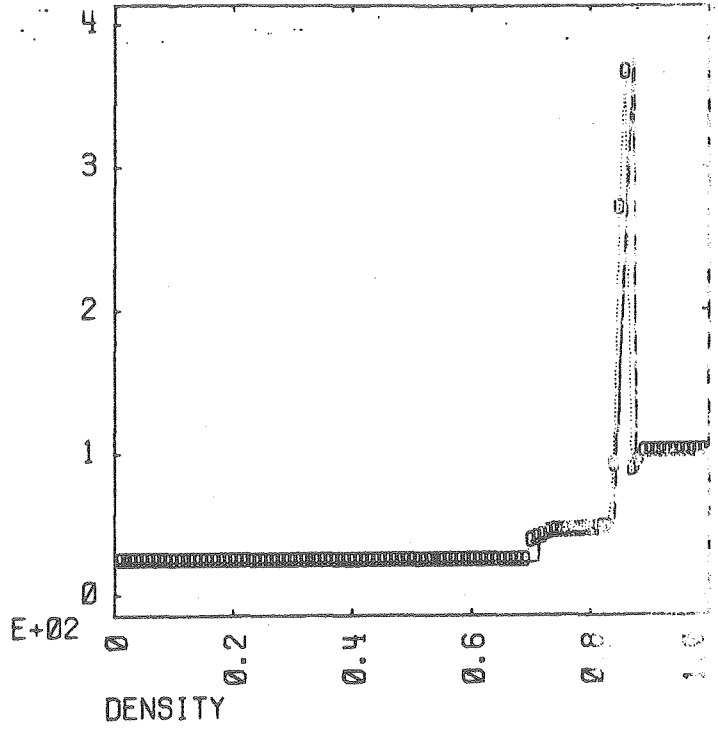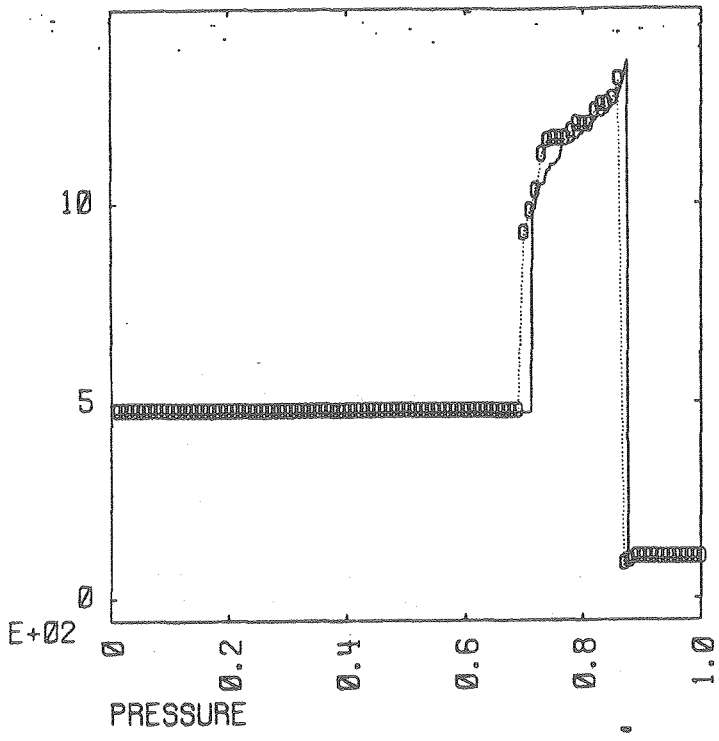
Figure 18.

Figure 19.

Figure 20.
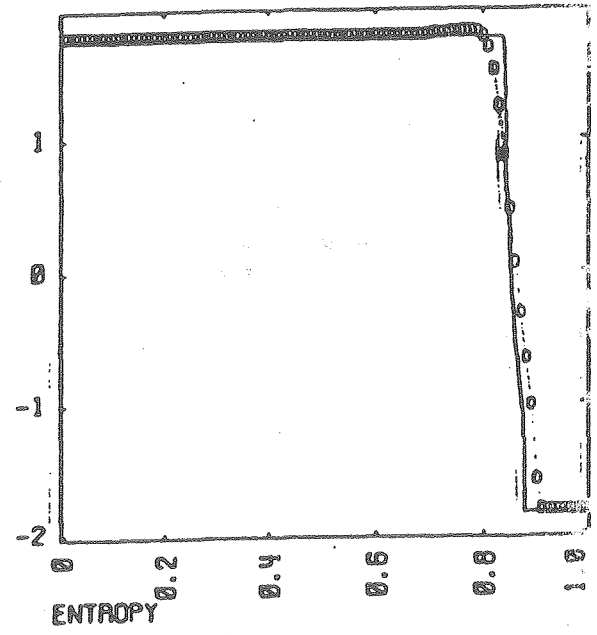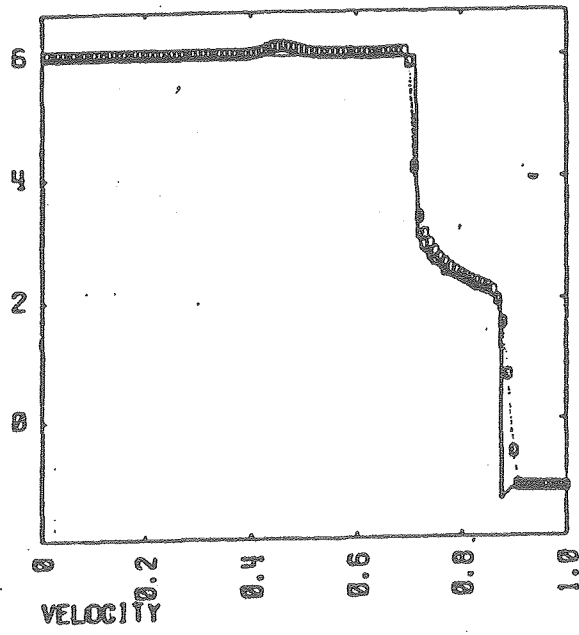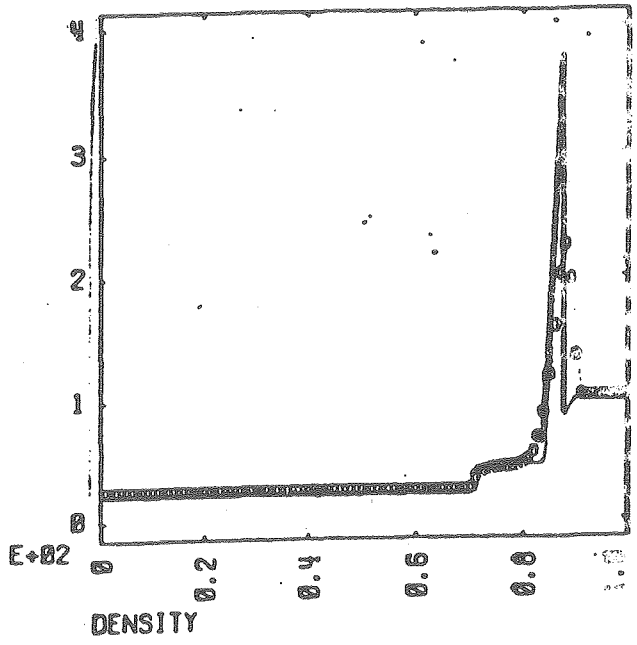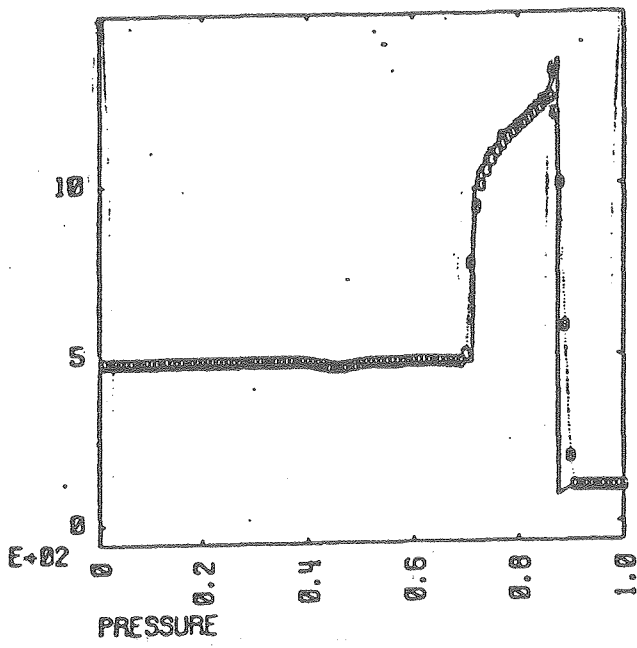
Figure 21.
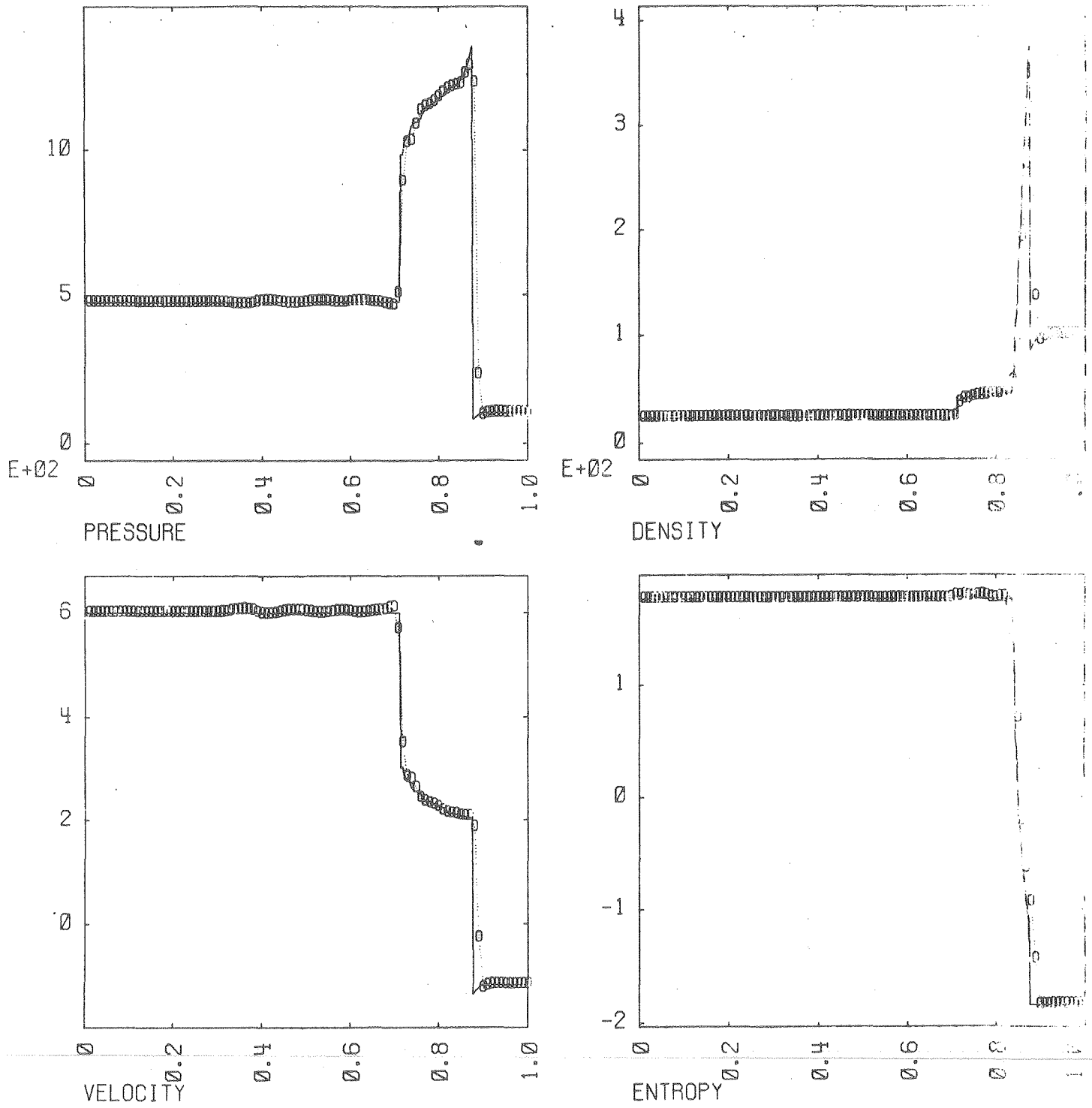
Figure 22.

Figure 23.

Figure A1.